

**CASE FILE
COPY**
**NATIONAL ADVISORY COMMITTEE
FOR AERONAUTICS**

TECHNICAL NOTE 2987

CHARTS RELATING THE COMPRESSIVE
BUCKLING STRESS OF LONGITUDINALLY SUPPORTED PLATES
TO THE EFFECTIVE DEFLECTIONAL AND ROTATIONAL
STIFFNESS OF THE SUPPORTS

By Roger A. Anderson and Joseph W. Semonian

Langley Aeronautical Laboratory
Langley Field, Va.



Washington
August 1953

NATIONAL ADVISORY COMMITTEE FOR AERONAUTICS

TECHNICAL NOTE 2987

CHARTS RELATING THE COMPRESSIVE
BUCKLING STRESS OF LONGITUDINALLY SUPPORTED PLATES
TO THE EFFECTIVE DEFLECTIONAL AND ROTATIONAL
STIFFNESS OF THE SUPPORTS

By Roger A. Anderson and Joseph W. Semonian

SUMMARY

A stability analysis is made of a long flat rectangular plate subjected to a uniform longitudinal compressive stress and supported along its longitudinal edges and along one or more other longitudinal lines by elastic line supports. The elastic supports possess deflectional and rotational stiffness. The results of the analysis are presented in the form of charts in which the buckling-stress coefficient is plotted against the buckle length of the plate for a wide range of support stiffnesses. The charts make possible the determination of the compressive buckling stress of plates supported by members whose stiffness may or may not be defined by elementary beam bending and twisting theory but yet whose effective restraint is amenable to evaluation. The deflectional and rotational stiffness provided by longitudinal stiffeners and full-depth webs is discussed and numerical examples are given to illustrate the application of the charts to the design of wing structures.

INTRODUCTION

In current thin-wing construction, thick cover plates are often supported or stiffened by thinner gage members whose stiffness determines the stability and strength of the cover plates. Experimental evidence is accumulating which indicates that, for certain longitudinal-stiffener proportions and for certain full-depth webs such as are found in multiweb construction, the supporting stiffness of these members must be carefully evaluated if reliable buckling stresses for the wing covers are to be calculated. The cross sections of these members often deform locally in a manner which permits deflection and rotation of the attached cover plate without developing the idealized beam or plate stiffness of the supporting member. For such construction, buckling stresses may not be predicted by stability criteria based upon beam stiffness quantities

such as EI for bending and GJ for torsion, or by criteria based upon an assumption of integral joints between cover plates and support members. The desirability of relating plate stability to a stiffness parameter which defines the actual or effective stiffness provided by the support is therefore evident.

The purpose of this paper is to present stability criteria for a number of supported-plate configurations frequently occurring in aircraft-wing construction in which criteria the theoretical elastic buckling-stress coefficient is given as a function of the buckle length of the plate for a range of effective deflectional or torsional stiffnesses of the supports. In order to use the criteria for a particular supported-plate configuration, the effective restraint provided by the supports must be amenable to evaluation. A section of the paper is devoted to a discussion of procedures for evaluation of the deflectional and torsional stiffness provided by longitudinal stiffeners and full-depth webs, including the effects of cross-sectional distortion. Numerical examples are then given which illustrate this evaluation for practical design problems. The derivations of the stability criteria are included in the appendixes.

SYMBOLS

b	width of plate between intermediate supports
λ	length of buckles
$\beta = \lambda/b$	
t	thickness of plate
x,y	coordinate axes in length and width directions, respectively
w	deflection normal to plane of plate
p	number of bays in width of plate
q	number of buckles occurring across width of plate
n	integer
a_n	Fourier coefficients
N	compressive load per unit width acting in x-direction (length direction) required to cause buckling

k nondimensional buckling-load coefficient, Nb^2/π^2D

σ compressive stress

σ_{cr} critical compressive stress

$$\varphi = \frac{\pi}{\beta} \sqrt{\beta\sqrt{k} - 1}$$

$$\theta = \frac{\pi}{\beta} \sqrt{\beta\sqrt{k} + 1}$$

E Young's modulus of elasticity

μ Poisson's ratio

D plate flexural stiffness per unit width, $\frac{Et^3}{12(1-\mu^2)}$

ψ deflectional stiffness per unit length of support, $lb/in.^2$

α rotational stiffness of intermediate support (moment per unit length required to produce a rotation of one radian)

γ rotational stiffness of edge support (moment per unit length required to produce a rotation of one radian)

$\frac{\psi b^3}{\pi^4 D}$ nondimensional deflectional restraint parameter

$\frac{ab}{\pi^2 D}, \frac{\gamma b}{\pi^2 D}$ nondimensional rotational restraint parameters

ϵ nondimensional rotational restraint parameter from reference 1

S, S^I, S^{II}, S^{IV} plate edge rotational stiffnesses defined in reference 2

C plate carry-over factor defined in reference 2

U_1, U_2, U_3 energies of deformation

V_1 work of applied stress

T	total potential energy of system
Q	energy parameter
$\Delta_1, \Delta_2, \Delta_3$	Lagrangian multipliers
A, B	coefficients defining amplitude of support deflection
A_s	cross-sectional area of stiffener
I_s	moment of inertia of stiffener cross section about its own center of gravity
Z_{pq}	modal coefficient affecting deflectional stiffness of longitudinal stiffener
$\frac{EI_{eff}}{bD}$	nondimensional bending stiffness parameter for stiffeners of sturdy cross section
c	ratio of average stress in stiffener to average stress in plate
P_{cr}	Euler column load
J	torsion constant
G	shear modulus of elasticity
C_{BT}	torsion coefficient which takes into account bending stiffness
I_p	polar moment of inertia
g	amplitude of sinusoidally distributed lateral load
$\delta(x)$	lateral deflection of longitudinally compressed stiffener subjected to sinusoidal lateral load
b_w	depth of web
t_w	thickness of web
D_w	plate flexural stiffness per unit width of web, $\frac{Et_w^3}{12(1 - \mu^2)}$

k_w	buckling-stress coefficient of web
z	distance between center of gravity of stiffener and middle plane of plate
ρ	radius of gyration of stiffener about its centroid

STATEMENT OF PROBLEM

In figure 1 are shown portions of several wing cross sections in which the material carrying bending stress is mainly concentrated in the thick plates forming the wing contour. Running spanwise are a number of lighter structural members in the form of longitudinal stiffeners and full-depth webs. In addition to carrying longitudinal stresses these members must resist cover-plate deflection and rotation at their respective locations by virtue of their stiffness. If the stiffness characteristics of these members can be defined, the buckling stress for the construction can be calculated.

In this analysis the assumption is made that longitudinal stiffeners and full-depth webs will provide a restraint to the attached cover plate which is proportional to the distortions of these support members. This condition is met if sinusoidally distributed normal loads or torsional moments on the supports are assumed to cause sinusoidally distributed distortions which are in phase with the loading. Thus support stiffness, which is the ratio of load intensity to distortion at any point, is a constant along the length of the support. With this support characteristic, the attached plate will buckle with deflections and rotations that are distributed sinusoidally in the length direction.

A cross section of the cover-plate buckling modes considered most likely to occur are sketched at the right of each wing cross section in figure 1 and are denoted cases 1 to 6. Cases 1, 2, and 3 primarily involve the deflectional stiffness characteristics of the support members, and cases 4, 5, and 6 involve the torsional stiffness characteristics of the supports. For a given wing cross section, both modes of buckling should be investigated to determine which mode leads to the lower buckling stress.

Cases 1 and 4 represent the buckling modes of a cover plate supported by substantial shear webs with an intermediate spanwise member (shown as a longitudinal stiffener) centrally located between the webs. The shear webs are assumed to prevent deflection but may offer a torsional restraint to the cover plate. In case 1 the stability of the compressed plate was investigated for a range of deflectional stiffnesses of the intermediate support and in case 4 the torsional stiffness of the

supports was considered. Because the two lowest buckling modes are either symmetrical or antisymmetrical with respect to the spanwise center line of the plate, it is not necessary to consider both the deflectional and rotational stiffness of the support simultaneously.

Cases 2 and 5 represent the most likely buckling modes for a cover plate with two equally spaced spanwise stiffening members of equal stiffness between shear webs. In case 2 the effect of support deflectional stiffness was investigated by assuming the torsional stiffness of the intermediate supports to be zero. The torsional stiffness of the intermediate supports was considered in case 5 with the assumption that the supports are capable of preventing plate deflection at their locations.

Cases 3 and 6 represent the most likely buckling modes for a plate stabilized by many spanwise lines of support of identical stiffness. These supports may be full-depth webs, as indicated in figure 1, or longitudinal stiffeners. In case 3, the deflectional stiffness of the supports was considered by assuming the support torsional stiffness to be zero. Torsional stiffness of the supports was considered in case 6 in which the deflections along the supports are assumed to be zero.

The loading and support conditions for the six cases considered are shown schematically in figure 2. The compression cover plate is represented by a uniformly compressed long flat plate which is simply supported at the loaded edges. The deflectional stiffness of the supports is represented by an elastic spring whose stiffness per unit length is denoted by ψ . The stiffness ψ may include the flexibility of the tension cover of the wing in those constructions where this flexibility would have an effect on the stability of the compression cover. The parameter ψ as defined in this paper is a generalization of the foundation modulus concept as used by Timoshenko for beams on an elastic foundation (ref. 3). The support torsional stiffness parameters are denoted by γ and α . The parameter γ is associated with the torsional stiffness of the nondeflecting shear webs and α is associated with the torsional stiffness of the intermediate supports. These two parameters are equivalent to the torsional stiffness parameter $4S_0$ defined by Lundquist and Stowell in reference 1.

For each of the first three cases a stability criterion in closed form is derived by the Lagrangian multiplier method (ref. 4). For the last three cases a stability criterion is obtained by using the principles of moment distribution explained in reference 2. With these stability criteria, numerical calculations have been made and are presented in design-chart form.

PRESENTATION OF STABILITY CRITERIA

Cases 1, 2, and 3.- The stability criteria for cases 1, 2, and 3 which involve the deflectional stiffness of the intermediate supports are presented in appendix A as equations (A19), (A24), and (A28). In these equations, the effective deflectional stiffness ψ of the supports is contained in the nondimensional parameter $\psi b^3/\pi^4 D$, and the effective torsional stiffness γ provided along the shear webs is contained in the nondimensional parameter $\gamma b/\pi^2 D$. Values of the parameter $\psi b^3/\pi^4 D$ may be determined from these equations as a function of the compressive buckling-stress coefficient $k = \frac{Nb^2}{\pi^2 D}$ and the ratio of buckle length to bay width λ/b for assigned values of the torsional restraint parameter $\gamma b/\pi^2 D$.

Two sets of numerical calculations have been made by assigning the values 0 and ∞ to $\gamma b/\pi^2 D$; these values correspond to simple support and complete fixity, respectively, along the shear webs. These numerical results are presented in tables I, II, and III. Cross plots of the values in the tables have been made to form design charts (figs. 3 to 7). From these charts, the combinations of $\psi b^3/\pi^4 D$, k , and λ/b at which buckling is initiated, may be read. The cutoffs in figures 5 and 7 define the values of $\psi b^3/\pi^4 D$ at which general instability involving deflection of the cover and the supports changes to local buckling of the cover (no support deflection) in accordance with the assumption made that the supports possess zero torsional stiffness.

In order to use the charts for plates on particular types of supports, the parameter $\psi b^3/\pi^4 D$ for the support must be evaluated. For the usual type of support, such as a longitudinal stiffener, or a full-depth web, $\psi b^3/\pi^4 D$ will be a function of the stresses in the support and the wave length of buckling, as well as the physical characteristics of the support. A discussion of the evaluation of $\psi b^3/\pi^4 D$ for longitudinal stiffeners and webs is given in the section entitled "Effective Stiffness of Supports," and numerical examples illustrating the procedure are given in a subsequent section entitled "Illustrative Examples."

Cases 4, 5, and 6.- For cases 4, 5, and 6, the cover is restrained by equally spaced nondeflecting supports of equal rotation stiffness α while the plate side edges are restrained by nondeflecting supports of equal rotational stiffness γ . The stability criteria for these cases are given in appendix B as equations (B2), (B6), and (B10). Values of the rotational stiffness parameter $\alpha b/\pi^2 D$ required to develop a given

compressive buckling-stress coefficient $k = \frac{Nb^2}{\pi^2 D}$ in the cover at a given ratio of buckle length to bay width λ/b may be determined from these equations for assigned values of the edge-restraint parameter $\gamma b/\pi^2 D$. As was done for the deflectional stiffness cases, numerical results are presented for $\gamma b/\pi^2 D$ equal to 0 and ∞ . The numerical results were obtained by using the stiffness tables of reference 5 and have been plotted to form design charts (figs. 8 to 12).

For a given design problem in which the supports have both deflectional and rotational stiffness, the buckling-stress coefficient obtained by considering the mode of buckling which involves the rotational stiffness of the supports must be compared with the coefficient obtained by considering the mode involving primarily the deflectional stiffness of the supports. The lower of these two values defines the buckling stress for the configuration. The evaluation of the torsional stiffness of longitudinal stiffeners and full-depth webs is discussed in the next section.

EFFECTIVE STIFFNESS OF SUPPORTS

General design charts have been presented, which, with one reservation, are independent of the medium providing restraint to the compression plate. The reservation is that the supporting medium must be of such a type that sinusoidally distributed normal loads and torsional moments cause sinusoidally distributed distortions which are in phase with the loading. Such behavior is characteristic of beam stiffness, as provided by longitudinal stiffeners of sturdy cross section. The distortions of the unstiffened webs during buckling of a multiweb beam also appear to be distributed sinusoidally along the length of the beam, and the reactions of the attachment flange on the compression cover of the beam are assumed to be proportional to the distortions.

A thorough analysis of the stiffness characteristics including effects of cross-sectional distortions and shear distortion of these two types of supports is beyond the scope of this paper; however, it is shown how these effects may be included in an evaluation of the stiffness parameters $\gamma b^3/\pi^4 D$ and $ab/\pi^2 D$.

Stiffness of longitudinal stiffeners.- The most common type of supporting medium for plates is the longitudinal stiffener which participates in carrying the compressive load. If the distortion characteristics of such a stiffener are defined by elementary beam bending theory, the deflection under a lateral load of amplitude g distributed sinusoidally over a length λ is

$$\delta(x) = \frac{\frac{g\lambda^4}{\pi^4 EI_{eff}} \sin \frac{\pi x}{\lambda}}{1 - \frac{\sigma A_s}{\frac{\pi^2 EI_{eff}}{\lambda^2}}}$$

where σA_s is the end load carried by the stiffener, and I_{eff} is the moment of inertia of the stiffener cross section about an axis lying in a plane parallel to the attached plate. The stiffness of the stiffener, defined as the ratio of lateral load to deflection, then is

$$\psi = \left(\frac{\pi}{\lambda}\right)^4 EI_{eff} \left(1 - \frac{\sigma A_s}{P_{cr}}\right) \quad (1)$$

If the average stress σ in the stiffener is proportional to the compressive buckling stress acting in the attached plate, ψ may be written as

$$\psi = \left(\frac{\pi}{\lambda}\right)^4 \left(EI_{eff} - ck \frac{A_s}{bt} \frac{\lambda^2}{b^2} bD\right)$$

or

$$\frac{\psi b^3}{\pi^4 D} = \left(\frac{b}{\lambda}\right)^4 \left(\frac{EI_{eff}}{bD} - ck \frac{A_s}{bt} \frac{\lambda^2}{b^2}\right) \quad (2)$$

where c is the ratio of the average stress in the stiffener to the average stress in the plate.

A recent theoretical analysis by Seide (ref. 6) shows that the effective moment of inertia of longitudinal stiffeners attached to one side of a uniformly compressed plate may be expressed as a correction to the moment of inertia of the stiffener about its own center of gravity I_s . In this form, equation (4) of reference 6 may be written

$$\frac{EI_{eff}}{bD} = \frac{EI_s}{bD} \left[1 + \frac{\left(\frac{z}{\rho}\right)^2}{1 + Z_{pq} \frac{A_s}{bt}} \right] \quad (3)$$

In equation (3) the quantity z is the distance between the center of gravity of the stiffener and the middle plane of the plate, and ρ is the radius of gyration of the stiffener. The modal coefficient Z_{pq} is a function of buckling mode and associated wave length. The variation of Z_{pq} with λ/b taken from reference 6 (which is applicable when the plate side edges are simply supported and when Poisson's ratio is $1/3$) is given in figure 13. The subscript p denotes the number of bays in the width of the plate, and q denotes the number of buckles across the width of the plate (q is equal to 1 for the cases considered in this paper). With EI_{eff}/bD defined, equation (2) should give satisfactory values of the stiffness parameter $\psi b^3/\pi^4 D$ for stiffeners of sturdy cross section; that is, stiffeners whose cross sectional and shearing distortions under load introduce deflections which are small compared with the over-all deflection as a beam.

In practical applications stiffeners are often formed from sheet, which necessitates a bend radius between the web of the stiffener and the flange for attachment to the sheet. For certain proportions, deflection of the plate may be appreciably increased by the flexibility of the attachment flange between the rivet line and the web of the stiffener, and by shearing distortion in the stiffener. If the total deflection δ is assumed equal to $\delta_1 + \delta_2 + \delta_3$ where δ_1 is the deflection due to bending of the stiffener as a beam, δ_2 is the deflection due to flexibility of the stiffener attachment flange, and δ_3 is the deflection due to shearing distortion in the stiffener, the effective stiffness may be written as

$$\frac{1}{\psi} = \frac{1}{\psi_1} + \frac{1}{\psi_2} + \frac{1}{\psi_3}$$

In nondimensional form the effective stiffness is given by

$$\frac{\psi b^3}{\pi^4 D} = \frac{1}{\frac{\pi^4 D}{\psi_1 b^3} + \frac{\pi^4 D}{\psi_2 b^3} + \frac{\pi^4 D}{\psi_3 b^3}} \quad (4)$$

where $\psi_1 b^3/\pi^4 D$ is given by the right-hand side of equation (2), $\psi_2 b^3/\pi^4 D$ must be evaluated either analytically or experimentally, and $\psi_3 b^3/\pi^4 D$ may be calculated. It is evident that if either ψ_1 , ψ_2 , or ψ_3 approaches zero, the effective stiffness of the stiffener approaches zero. Any other significant distortions can be included in a similar manner.

The torsional restraint furnished a plate by a stiffener which undergoes no cross-sectional distortion when it twists is discussed in reference 7. The expression for its stiffness (eq. (8) of ref. 7 rewritten in the notation of the present paper) is

$$\alpha = \frac{\pi^2}{\lambda^2} \left(GJ + \frac{\pi^2}{\lambda^2} EC_{BT} - \sigma I_p \right)$$

where the quantities J , C_{BT} , and I_p must be calculated with respect to an assumed axis of rotation. In nondimensional form, the stiffness is

$$\frac{ab}{\pi^2 D} = \left(\frac{b}{\lambda} \right)^2 \left(\frac{GJ}{bd} + \pi^2 \frac{b^2}{\lambda^2} \frac{EC_{BT}}{b^3 D} - c k \pi^2 \frac{I_p}{b^3 t} \right) \quad (5)$$

Expressions similar to equation (5) should be derived for those stiffeners in which torsional moments applied to the stiffener attachment flange cause distortion of the cross section of the stiffener when it twists.

Stiffness of full-depth webs. - When the compression cover of a beam is supported by full-depth webs as in a multiweb beam, the effective stiffness of the webs in resisting sheet deflection and rotation at the sheet-web juncture must be evaluated. Reference 8, for example, evaluates the effectiveness of integrally joined webs as torsional restraints on the cover of a multiweb beam. The assumption made in that analysis is that the webs possess sufficient deflectional stiffness to form longitudinal nodes along the sheet-web juncture during buckling. The range of sheet and web proportions for which this assumption is valid, however, is not established.

For built-up construction, the deflectional stiffness provided by an unstiffened web plate is influenced by the eccentricity of the connection between web and cover plates and by the state of stress existing in the webs of a beam under load. In particular, for channel-type webs

formed from sheet, appreciable distortions of the attachment flanges and lateral deflection of the web are produced by either depthwise crushing or stretching forces. In accordance with the stiffness analysis for longitudinal stiffeners, the stiffness of the channel should be analyzed under the action of a depthwise load applied sinusoidally along the length of the attachment flange in the presence of the stresses that exist in the web during beam bending. This procedure is illustrated by a numerical example in the next section. The outcome of such an analysis is influenced rather strongly by the assumed eccentricity of the applied load (with respect to the plane of the web) and by the degree of clamping that is assumed to be provided by the riveted connection between web attachment flanges and the cover plates. The importance of these factors in calculating deflectional stiffnesses has been emphasized by Bijlaard and Johnston in a recent paper (ref. 9).

With regard to the torsional restraint provided to the compression cover by integrally joined webs, the restraint data presented in figure 9 of reference 8 are analogous to equation (5) for the torsional stiffness of a stiffener; that is, the restraint coefficient ϵ in figure 9 of reference 8 is a measure of the negative of the stiffness of a web subjected to a pure bending stress distribution as a function of buckle length. The relationship between the torsional stiffness parameter ab/π^2D of the present paper and the restraint coefficient ϵ is

$$\frac{ab}{\pi^2 D} = - \frac{\epsilon}{\pi^2} \frac{b}{b_W} \frac{D_W}{D} \quad (6)$$

When webs are not integrally joined to the cover, the stiffness of the attachment should be taken into account when the parameter ab/π^2D is calculated.

ILLUSTRATIVE EXAMPLES

Some of the procedures outlined in the preceding section for calculating the effective stiffness of supports will be illustrated in the solution of two common cover-plate stability problems. The first example chosen considers the type of restraint offered by the webs of a multiweb structure and the second considers the effect of one sided longitudinal stiffeners on plate buckling.

Buckling of a multiweb structure.-- When the webs used in a multiweb wing are formed from sheet metal there is no assurance that the deflectional restraint provided to the beam covers by the formed channel webs

is sufficient to form longitudinal nodes along the web lines and thus to force buckling of the type denoted as case 6. The subsequent calculations illustrate a simple procedure that may be used to investigate the possible occurrence of buckling in the mode denoted as case 3. The calculations apply to a multiweb beam tested in pure bending in the combined load testing machine of the Langley structures research laboratory. The beam had four identical channel webs (3 cells) and it is assumed that the analysis for a beam with an infinite number of cells can be applied. The physical dimensions of the beam are as follows:

Cover width between webs, b, in.	3.75
Cover thickness, t, in.	0.125
Channel web depth, b_w , in.	2.08
Channel web thickness, t_w , in.	0.050
Bend radius between web and attachment flange, in.	0.20
Diameter of web-attachment rivets, in.	3/16
Pitch of web-attachment rivets, in.	9/16
Distance between midplane of web and rivet line of attachment to cover, f (attachment flange assumed to be effectively clamped to cover at the inner edge of the rivet shanks when closely spaced rivets are used), in.	0.36
Young's modulus for the 75S-T6 aluminum alloy, psi	10.5×10^6
Poisson's ratio for the material	0.333

In accordance with the procedure outlined in the preceding section, the deflectional stiffness of the channel must be evaluated under the action of a sinusoidally distributed lateral load of amplitude g on the channel web in the presence of the existing bending stresses. This loading is shown in figure 14(a). The lateral loading is applied a distance f from the web plane, the distance at which the flange has been assumed to be completely fixed to the cover plate. In order to compute the deflection at a given cross section, the channel is idealized as in figure 14(b). The attachment flange is cut from the web and assumed to be flat and to be free of longitudinal compression stress. (This stress is usually small in relation to the critical buckling stress of that portion of the flange between the rivet line and the web.) Also, since the buckle length is large compared with the distance f , the longitudinal bending stiffness of the flange will be neglected in computing the distortions at a given cross section. These distortions are shown in figure 14(c). The left-hand edge of the attachment flange is free but maintains a zero slope (to match the slope of the attached plate when buckling occurs in the mode denoted as case 3), whereas the right-hand edge is supported against deflection and elastically restrained against rotation by the torsional restraint α' . The restraint α' represents the resistance to rotation which the web offers the flange and is a function of both buckle length and the bending stress in the web. Because of the flexible corner radius that actually exists between the attachment flange and the web, the beam

cover is assumed to be equally free to deflect up or down with the attachment flange. Simple tension and compression loading tests on channels with corner radii verify this assumption. With these simplifying assumptions and boundary conditions, the deflection δ at any cross section may be written

$$\delta(x) = \frac{gf^3}{12D_W} \frac{1 + 4 \frac{D_W}{\alpha'f}}{1 + \frac{D_W}{\alpha'f}} \sin \frac{\pi x}{\lambda}$$

The effective stiffness of the channel, defined as the ratio of lateral load to deflection, then is

$$\psi = \frac{12D_W}{f^3} \frac{1 + \frac{D_W}{\alpha'f}}{1 + 4 \frac{D_W}{\alpha'f}}$$

or in nondimensional form

$$\frac{\psi b^3}{\pi^4 D} = \frac{\frac{12}{\pi^4} \left(\frac{t_W}{t}\right)^3 \frac{f}{b_W} \epsilon - 1}{\left(\frac{f}{b_W}\right)^3 \left(\frac{b_W}{b}\right)^3 \frac{f}{b_W} \epsilon - 4} \quad (7)$$

where ϵ is the restraint parameter from figure 9 of reference 8 and is defined as

$$\epsilon = - \frac{\alpha' b_W}{D_W}$$

Substitution of the physical dimensions of the beam into equation (7) for $\psi b^3/\pi^4 D$ gives

$$\frac{\psi b^3}{\pi^4 D} = 8.93 \frac{0.173\epsilon - 1}{0.173\epsilon - 4} \quad (8)$$

In order to obtain numerical values for $\psi b^3/\pi^4 D$, the quantity ϵ must be read from figure 9 of reference 8. Values of ϵ may be obtained which are compatible with the bending stress distribution in the beam if the stress in the extreme fiber of the web is assumed to be equal to the average stress in the beam covers and the lengths of the buckles in the webs and covers are equal. From these two conditions, the following equations result:

$$k_w = k \left(\frac{b_w}{b} \right)^2 \left(\frac{t}{t_w} \right)^2 = 1.92k \quad (9)$$

$$\frac{\lambda}{b_w} = \frac{\lambda}{b} \frac{b}{b_w} = 1.80 \frac{\lambda}{b} \quad (10)$$

The lowest value of the buckling-stress coefficient k which simultaneously satisfied equations (8), (9), and (10) is the desired value and is found by a trial and error procedure.

The first step in this procedure consists in determining by trial and error the value of k which satisfied equations (8), (9), and (10) for an assumed value of λ/b . Values of ϵ are read from the curves of figure 9 of reference 8, and values of $\psi b^3/\pi^4 D$ are read from figure 7 of this paper. This procedure is repeated for several assumed values of λ/b . If this procedure is used, values of k equal to 3.35, 3.25, 3.26, and 3.47 are found for assumed values of λ/b equal to 0.7, 0.8, 0.9, and 1.0, respectively. The final step is to minimize k with respect to λ/b . The minimum value of k for this mode of buckling (case 3) is thus found to be 3.24 at $\frac{\lambda}{b} = 0.85$.

In order to determine the buckling-stress coefficient that would be obtained with buckling of the type denoted as case 6, figure 2 of reference 8 may be used to read the buckling-stress coefficient directly. The use of this direct-reading chart involves an assumption of an integral joint between the webs and the covers, and the indicated k value is 4.1, which is considerably higher than the value 3.24 previously obtained.

The actual experimental values of the buckling and failure stress for the example beam were

$$\sigma_{cr} = 33,400 \text{ psi}$$

$$\sigma_{failure} = 36,600 \text{ psi}$$

and the mode of buckling observed was that of the case 3. If the value $k = 3.24$ is substituted into the familiar buckling equation

$$\sigma_{cr} = \frac{k\pi^2 E}{12(1 - \mu^2)} \left(\frac{t}{b}\right)^2$$

a buckling stress of 34,800 psi is obtained.

Buckling of a plate with one-sided stiffeners. - In calculations of the buckling stress for plates with stiffeners attached to one side, the assumption is commonly made that the moment of inertia of the stiffeners may be calculated about the plane of attachment to the plate. The following example illustrates the procedure for obtaining the buckling stress of the plate-stiffener combination when this assumption is made and also the slight variation in the procedure which is entailed by using the expression from reference 6 for the effective moment of inertia of a one-sided stiffener.

Consider the effect of two equally spaced longitudinal stiffeners of sturdy cross section on the stability of a long compressed plate which is simply supported along the unloaded edges and supported by deflectionally rigid transverse ribs at equal intervals along the length. Assume that the stiffeners and ribs offer no torsional restraints to the plate. The following physical dimensions are given:

Plate thickness, t, in.	0.188
Plate width between stiffeners, b, in.	4.70
Rib spacing, in.	30
Cross sectional area of 1/8-inch thick Z-stiffener, As, sq in.	0.431
Moment of inertia of stiffener about its centroid, I_s , in. ⁴	0.203
Radius of gyration of stiffener, ρ , in.	0.686
Moment of inertia of stiffener about plane of attachment to sheet, in. ⁴	0.524
Distance between centroid of stiffener and centroid of plate, z, in.	0.956
Young's modulus for the 75S-T6 aluminum alloy, psi	10.5×10^6
Poisson's ratio for the material	0.333

The deflectional stiffness of a longitudinal stiffener of sturdy cross section is given by (see eq. (2))

$$\frac{\psi b^3}{\pi^4 D} = \left(\frac{b}{\lambda}\right)^4 \left(\frac{EI_{eff}}{bD} - k \frac{A_s}{bt} \frac{\lambda^2}{b^2} \right)$$

if the compressive stress in the plate and stiffener are equal. If EI_{eff} is calculated about the plane of attachment of stiffener to sheet, $\frac{EI_{eff}}{bD}$ is

$$\frac{EI_{eff}}{bD} = \frac{12 [1 - (0.33)^2] (0.524) E}{(4.70)(0.188)^3 E} = 179$$

If the buckle length is taken to be the rib spacing, the numerical expression for $\psi b^3 / \pi^4 D$ is

$$\frac{\psi b^3}{\pi^4 D} = \left(\frac{4.70}{30}\right)^4 \left[179 - \frac{0.431}{4.70 \times 0.188} \left(\frac{30}{4.70}\right)^2 k \right]$$

$$= 0.1080 - 0.01195 k$$

The value of k which satisfies this equation simultaneously with the curves of figure 5 at $\frac{\lambda}{b} = \frac{30}{4.70}$ is the desired value. By trial and error, a common solution is found at $k = 3.55$. In order to verify that $k = 3.55$ is the lowest buckling-stress coefficient, the analysis is repeated by assuming that two buckles occur between rib stations. In this particular example, this assumption leads to a much higher value of k .

The buckling-stress coefficient is now computed by assuming that $\frac{EI_{eff}}{bD}$ is given by

$$\frac{EI_{eff}}{bD} = \frac{EI_s}{bD} \left[1 + \frac{\left(\frac{z}{p}\right)^2}{1 + Z_{pq} \frac{A_s}{bt}} \right]$$

In order that the modal coefficient Z_{pq} may be read from the curves of figure 13, the buckle length must be assumed. The previous calculation indicated that the length of the buckle is 30 inches and that it extends across the entire width of the plate. Thus, with $p = 3$, $q = 1$, and $\frac{\lambda}{b} = \frac{30}{4.70}$, the value of Z_{pq} read from figure 13 is 0.80.

From the data previously given, $\frac{EI_{eff}}{bD}$ is then

$$\frac{EI_{eff}}{bD} = \frac{12 [1 - (0.333)^2] (0.203) E}{4.70 (0.188)^3 E} \left[1 + \frac{\left(\frac{0.956}{0.686}\right)^2}{1 + \frac{0.80 \times 0.431}{4.70 \times 0.188}} \right]$$

$$= (69.4)(2.394) = 166.0$$

With this value for $\frac{EI_{eff}}{bd}$ the expression for $\psi b^3/\pi^4 D$ is

$$\frac{\psi b^3}{\pi^4 D} = 0.100 - 0.01195k$$

By the use of figure 5, the value found for k is 3.25. This value is about 8 percent lower than the value 3.55 obtained when the moment of inertia was rather arbitrarily chosen. (For other plate-stiffener combinations, the difference in the k values calculated by these two procedures can be either larger or smaller than the difference obtained in this numerical example.)

The buckling stress for the stiffened plate is found by substituting the value of $k = 3.25$ into the buckling equation and a buckling stress of 50,400 psi for 75S-T6 aluminum alloy is predicted.

CONCLUDING REMARKS

Design charts have been presented which permit the evaluation of the compressive buckling stress of a long flat rectangular plate with various deflectional and rotational elastic line supports running lengthwise of the plate. In order to use the charts in a particular plate buckling problem, the restraint provided by supporting elements such as angle and z-sections and full-depth webs like those used in multiweb wing construction must be evaluated. The evaluation of the stiffness of these supports has been discussed, and possible approaches for obtaining the required stiffnesses are presented. Numerical examples have been included to illustrate the type of procedures involved in computing buckling stresses.

Langley Aeronautical Laboratory,
 National Advisory Committee for Aeronautics,
 Langley Field, Va., June 5, 1953.

APPENDIX A

DERIVATION OF STABILITY CRITERIA FOR CASES 1, 2, AND 3

Although a set of stability criteria could be derived for the general case involving any number of lines of support either by solving the plate differential equation or by the Rayleigh-Ritz energy method, a desirable gain in simplicity is achieved by applying the energy method using Lagrangian multipliers (see ref. 4) to the individual cases. The latter approach is shown in some detail for case 1, and variations in the method are indicated for cases 2 and 3.

Case 1. - An exact representation of the buckle pattern for case 1 is given by the following series

$$w = \sin \frac{\pi x}{\lambda} \sum_{n=1,3,5}^{\infty} a_n \sin \frac{n\pi y}{2b} \quad (A1)$$

where the origin of the coordinate system lies along a side edge of the plate. The sinusoidal deflection along the plate center line may be written as

$$w(x,b) = A \sin \frac{\pi x}{\lambda} \quad (A2)$$

and the slope along the side edges of the plate may be written as

$$\frac{\partial w}{\partial y}(x,0) = B \frac{\pi}{2b} \sin \frac{\pi x}{\lambda} \quad (A3)$$

Compatibility of equations (A1), (A2), and (A3) requires that

$$\left. \begin{aligned} \sum_{n=1,3,5}^{\infty} a_n \sin \frac{n\pi}{2} - A &= 0 \\ \sum_{n=1,3,5}^{\infty} a_n n - B &= 0 \end{aligned} \right\} \quad (A4)$$

Using equation (A1) permits the so-called strain energy of bending stored in the buckled plate to be written as

$$U_1 = \frac{D}{2} \int_0^\lambda \int_0^{2b} \left(\frac{\partial^2 w}{\partial x^2} + \frac{\partial^2 w}{\partial y^2} \right)^2 dx dy = \frac{D}{4} \pi^4 \lambda b \sum_{n=1,3,5}^{\infty} a_n^2 \left(\frac{1}{\lambda^2} + n^2 \frac{1}{4b^2} \right)^2 \quad (A5)$$

Using equation (A2) gives the energy stored in the deflectional restraint as

$$U_2 = \frac{\psi}{2} \int_0^\lambda [w(x, b)]^2 dx = \frac{\psi}{4} \lambda A^2 \quad (A6)$$

and using equation (A3) gives the energy stored in the torsional restraints as

$$U_3 = 2 \frac{\gamma}{2} \int_0^\lambda \left[\frac{\partial w}{\partial y}(x, 0) \right]^2 dx = \frac{\gamma}{2} \left(\frac{\pi}{2b} \right)^2 \lambda B^2 \quad (A7)$$

The so-called external work done by the uniform compressive load N at buckling is

$$V_1 = \frac{N}{2} \int_0^\lambda \int_0^{2b} \left(\frac{\partial w}{\partial x} \right)^2 dx dy = \frac{N}{4} \pi^2 \frac{b}{\lambda} \sum_{n=1,3,5}^{\infty} a_n^2 \quad (A8)$$

The total potential energy may now be written as

$$T = (U_1 + U_2 + U_3 - V_1)$$

or

$$T' = 4 \frac{\lambda b}{\pi^4 D} T = \sum_{n=1,3,5}^{\infty} a_n^2 \left[\left(\frac{1}{\beta} + \frac{n^2}{4} \beta \right)^2 - k \right] + \frac{\psi b^3}{\pi^4 D} \beta^2 A^2 + \frac{1}{2} \frac{\gamma b}{\pi^2 D} \beta^2 B^2 \quad (A9)$$

where $\beta = \frac{\lambda}{b}$, $k = \frac{Nb^2}{\pi^2 D}$, and $\frac{\psi b^3}{\pi^4 D}$ and $\frac{\gamma b}{\pi^2 D}$ are the nondimensional deflectional stiffness and rotational stiffness parameters, respectively.

The buckling load is determined by the condition that the potential energy T' must be a minimum. Since the coefficients A and B depend upon the Fourier coefficients, a_n , the expression to be minimized, is

$$Q = T' - \Delta_1 \left(\sum_{n=1,3,5}^{\infty} a_n \sin \frac{n\pi}{2} - A \right) - \Delta_2 \left(\sum_{n=1,3,5}^{\infty} a_n n - B \right) \quad (A10)$$

where Δ_1 and Δ_2 are the Lagrangian multipliers. The potential energy T' is a minimum when

$$\frac{\partial Q}{\partial a_n} = \frac{\partial Q}{\partial A} = \frac{\partial Q}{\partial B} = \frac{\partial Q}{\partial \Delta_1} = \frac{\partial Q}{\partial \Delta_2} = 0 \quad (A11)$$

$$\frac{\partial Q}{\partial a_n} = 2a_n \left[\left(\frac{1}{\beta} + \frac{n^2}{4} \beta \right)^2 - k \right] - \Delta_1 \sin \frac{n\pi}{2} - \Delta_2 n = 0 \quad (n = 1, 3, 5, \dots, \infty) \quad (A12)$$

$$\frac{\partial Q}{\partial A} = 2A \frac{\psi b^3}{\pi^4 D} \beta^2 + \Delta_1 = 0 \quad (A13)$$

$$\frac{\partial Q}{\partial B} = B \frac{\gamma b}{\pi^2 D} \beta^2 + \Delta_2 = 0 \quad (A14)$$

$$\frac{\partial Q}{\partial \Delta_1} = \sum_{n=1,3,5}^{\infty} a_n \sin \frac{n\pi}{2} - A = 0 \quad (A15)$$

$$\frac{\partial Q}{\partial \Delta_2} = \sum_{n=1,3,5}^{\infty} a_n n - B = 0 \quad (A16)$$

Equations (A12), (A13), and (A14) may be solved for a_n , A, and B, respectively, and these expressions substituted into the compatibility conditions (eqs. (A15) and (A16)). This substitution results in the following two simultaneous homogeneous equations:

$$\frac{\Delta_1}{2} \left\{ \frac{1}{\beta^2 \frac{\gamma b}{\pi^2 D}} + \sum_{n=1,3,5}^{\infty} \frac{\sin^2 \frac{n\pi}{2}}{\left(\frac{1}{\beta} + \frac{n^2}{4} \beta\right)^2 - k} \right\} + \frac{\Delta_2}{2} \sum_{n=1,3,5}^{\infty} \frac{n \sin \frac{n\pi}{2}}{\left(\frac{1}{\beta} + \frac{n^2}{4} \beta\right)^2 - k} = 0 \quad (A17)$$

$$\frac{\Delta_1}{2} \sum_{n=1,3,5}^{\infty} \frac{n \sin \frac{n\pi}{2}}{\left(\frac{1}{\beta} + \frac{n^2}{4} \beta\right)^2 - k} + \frac{\Delta_2}{2} \left\{ \frac{2}{\beta^2 \frac{\gamma b}{\pi^2 D}} + \sum_{n=1,3,5}^{\infty} \frac{n^2}{\left(\frac{1}{\beta} + \frac{n^2}{4} \beta\right)^2 - k} \right\} = 0 \quad (A18)$$

Each of the infinite sums in equations (A17) and (A18) are amenable to exact evaluation. Resolving the infinite series in equations (A17) and (A18) into partial fractions yields the following forms:

$$\sum_{n=1,3,5}^{\infty} \frac{\sin^2 \frac{n\pi}{2}}{\left(\frac{1}{\beta} + \frac{n^2}{4} \beta\right)^2 - k} = \frac{2}{\beta \sqrt{k}} \sum_{n=1,3,5}^{\infty} \frac{1}{n^2 - \frac{4}{\pi^2} \phi^2} - \frac{2}{\beta \sqrt{k}} \sum_{n=1,3,5}^{\infty} \frac{1}{n^2 + \frac{4}{\pi^2} \theta^2}$$

$$\sum_{n=1,3,5}^{\infty} \frac{n^2}{\left(\frac{1}{\beta} + \frac{n^2}{4} \beta\right)^2 - k} = \frac{8\beta\phi^2}{\pi^2\sqrt{k}} \sum_{n=1,3,5}^{\infty} \frac{1}{n^2 - \frac{4}{\pi^2} \phi^2} + \frac{8\beta\theta^2}{\pi^2\sqrt{k}} \sum_{n=1,3,5}^{\infty} \frac{1}{n^2 + \frac{4}{\pi^2} \theta^2}$$

$$\sum_{n=1,3,5}^{\infty} \frac{n \sin \frac{n\pi}{2}}{\left(\frac{1}{\beta} + \frac{n^2}{4} \beta\right)^2 - k} = \frac{2\beta}{\sqrt{k}} \sum_{n=1,2,3}^{\infty} \frac{(-1)^{n-1} n \sin \frac{n\pi}{2}}{n^2 - \frac{4}{\pi^2} \varphi^2} -$$

$$\frac{2\beta}{\sqrt{k}} \sum_{n=1,2,3}^{\infty} \frac{(-1)^{n-1} n \sin \frac{n\pi}{2}}{n^2 + \frac{4}{\pi^2} \theta^2}$$

where

$$\varphi = \frac{\pi}{\beta} \sqrt{\beta \sqrt{k} - 1}$$

$$\theta = \frac{\pi}{\beta} \sqrt{\beta \sqrt{k} + 1}$$

By using equation (6.495) of reference 10, the infinite series can be written in closed form. Thus,

$$\sum_{n=1,3,5}^{\infty} \frac{\sin^2 \frac{n\pi}{2}}{\left(\frac{1}{\beta} + \frac{n^2}{4} \beta\right)^2 - k} = \frac{\pi^2}{4\beta\sqrt{k}} \left(\frac{1}{\varphi} \tan \varphi - \frac{1}{\theta} \tanh \theta \right)$$

$$\sum_{n=1,3,5}^{\infty} \frac{n^2}{\left(\frac{1}{\beta} + \frac{n^2}{4} \beta\right)^2 - k} = \frac{1}{\beta\sqrt{k}} (\varphi \tan \varphi + \theta \tanh \theta)$$

$$\sum_{n=1,3,5}^{\infty} \frac{n \sin \frac{n\pi}{2}}{\left(\frac{1}{\beta} + \frac{n^2}{4} \beta\right)^2 - k} = \frac{\pi}{2\beta\sqrt{k}} \left(\frac{1}{\cos \varphi} - \frac{1}{\cosh \theta} \right)$$

Substituting the closed forms of the infinite series into equations (A17) and (A18) and simplifying yield the following stability criterion:

$$0 = \begin{vmatrix} \frac{4}{\pi^2} \left(\varphi^2 \frac{\sin \varphi}{\cos \varphi} + \theta^2 \frac{\sinh \theta}{\cosh \theta} \right) + \frac{\delta \sqrt{k}}{\pi^2 \beta} & \frac{2}{\pi} \left(\frac{1}{\cos \varphi} - \frac{1}{\cosh \theta} \right) \\ \frac{2}{\pi} \left(\frac{1}{\cos \varphi} - \frac{1}{\cosh \theta} \right) & \left(\frac{\sin \varphi}{\cos \varphi} - \frac{\sinh \theta}{\cosh \theta} \right) + \frac{4\sqrt{k}}{\pi^2 \beta} \frac{\psi b^3}{\pi^4 D} \end{vmatrix} \quad (\text{A19})$$

For given values of k , β , and $\psi b^3/\pi^4 D$, the value of $\psi b^3/\pi^4 D$ which causes the determinant to vanish is the desired value. When the side edges of the plate are simply supported, which is equivalent to setting $\frac{\psi b^3}{\pi^4 D} = 0$, the criterion reduces to

$$\frac{\psi b^3}{\pi^4 D} = \frac{\frac{4\sqrt{k}}{\pi^2 \beta}}{\frac{\sin \varphi}{\cos \varphi} - \frac{\sinh \theta}{\cosh \theta}} \quad (\text{A20})$$

In reference 11, a stability criterion is presented for the compressive buckling of simply supported plates with an arbitrary number of longitudinal stiffeners. When equation (A7) of reference 11 is applied to an infinitely long plate and written in the notation of the present paper it appears as

$$\frac{1}{\beta^4} \left(\frac{EI_{eff}}{bd} - k \frac{A_s}{bt} \beta^2 \right) = \frac{\frac{4\sqrt{k}}{\pi^2 \beta}}{\frac{\sin \varphi}{\varphi} - \frac{\sinh \theta}{\theta}} - \frac{\cos \frac{\pi q}{p} - \cos \varphi}{\cos \frac{\pi q}{p} - \cosh \theta}$$

which is equivalent to

$$\frac{\psi b^3}{\pi^4 D} = \frac{\frac{4\sqrt{k}}{\pi^2 \beta}}{\frac{\sin \varphi}{\varphi} - \frac{\sinh \theta}{\theta}} - \frac{\cos \frac{\pi q}{p} - \cos \varphi}{\cos \frac{\pi q}{p} - \cosh \theta} \quad (A21)$$

when the stiffness of a stiffener is defined by elementary beam theory and the stresses in the plate and the stiffener are equal (see eq. (2)). Equation (A21) may be used for plates with simply supported side edges and with an arbitrary number of longitudinal supports. Equation (A20) may be obtained from equation (A21) by substitution of the proper values of p and q for case 1; that is, $p = 2$ and $q = 1$.

For complete fixity of the side edges, $\frac{\gamma b}{\pi^2 D} = \infty$, the stability criterion (eq. (A19)) reduces to

$$\frac{\psi b^3}{\pi^4 D} = \frac{\frac{4\sqrt{k}}{\pi^2 \beta}}{\left(\frac{\sinh \theta}{\theta} - \frac{\sin \varphi}{\varphi} \right) + \frac{\left(\frac{1}{\cos \varphi} - \frac{1}{\cosh \theta} \right)^2}{\theta^2 \frac{\sinh \theta}{\theta} + \frac{\varphi^2 \sin \varphi}{\varphi}}} \quad (A22)$$

Solutions of these equations and those to follow are facilitated by a tabulation of the functions φ , $\sin \varphi$, $\cos \varphi$, θ , $\sinh \theta$, $\cosh \theta$ for appropriate values of the parameters k and β . These data are provided in table IV.

Case 2.- An exact representation of the deflection for case 2 is given by

$$w = \sin \frac{\pi x}{\lambda} \sum_{n=1,2,3}^{\infty} a_n \sin \frac{n\pi y}{\beta b} \quad (A23)$$

Following the same procedure as for case 1, two criteria are obtained, one for symmetrical buckling and one for an antisymmetrical wave pattern. Calculations made by considering both modes of buckling indicated that, except for a very limited combination of values of k and λ/b ($k \geq 4$ and λ/b in the neighborhood of unity), buckling in a symmetrical mode requires the highest values of the stiffness parameter $\psi b^3/\pi^4 D$ to achieve a given buckling-stress coefficient k . Thus, for most practical problems, the criterion for symmetrical buckling only need be considered and is given in determinant form:

$$\left| \begin{array}{l} - \frac{9}{\pi^2} \left(p^2 \frac{1+2\cos\varphi}{1+\cos\varphi} \frac{\sin\varphi}{\frac{1}{2}-\cos\varphi} + q^2 \frac{1+2\cosh\theta}{1+\cosh\theta} \frac{\sinh\theta}{\frac{1}{2}-\cosh\theta} \right) + \frac{36\sqrt{k}}{\pi^2 \beta} \\ \frac{3}{\pi} \left(\frac{\theta}{\sinh\theta} \frac{\sinh\theta}{\frac{1}{2}-\cosh\theta} - \frac{\varphi}{\sin\varphi} \frac{\sin\varphi}{\frac{1}{2}-\cos\varphi} \right) \\ \frac{3}{\pi} \left(\frac{\theta}{\sinh\theta} \frac{\sinh\theta}{\frac{1}{2}-\cosh\theta} - \frac{\varphi}{\sin\varphi} \frac{\sin\varphi}{\frac{1}{2}-\cos\varphi} \right) - \frac{3}{\pi} \left(\frac{\theta}{\sinh\theta} \frac{\sinh\theta}{\frac{1}{2}-\cosh\theta} - \frac{\varphi}{\sin\varphi} \frac{\sin\varphi}{\frac{1}{2}-\cos\varphi} \right) \end{array} \right| = 0 \quad (A24)$$

When the plate side edges are simply supported, the criterion reduces to

$$\frac{\psi b^3}{\pi^4 D} = \frac{\frac{4\sqrt{k}}{\pi^2 \beta}}{\frac{\sin\varphi}{\varphi} - \frac{\sinh\theta}{\theta}} \quad (A25)$$

$$\frac{\frac{1}{2}-\cos\varphi}{\frac{1}{2}-\cosh\theta}$$

which is the same as equation (A21) for $q = 1$, $p = 3$.

For complete fixity of the side edges, the criterion is

$$\frac{\frac{4\sqrt{k}}{\pi^2 \beta}}{\frac{\sin \varphi}{\varphi} - \frac{\sinh \theta}{\theta} - \frac{\left(\frac{\theta}{\sinh \theta} \frac{\sinh \theta}{\frac{1}{2} - \cosh \theta} - \frac{\varphi}{\sin \varphi} \frac{\sin \varphi}{\frac{1}{2} - \cos \varphi} \right)^2}{\frac{1}{2} - \cosh \theta \frac{1}{2} - \cosh \theta \frac{\sinh \theta}{\theta^2 \frac{1 + 2 \cosh \theta}{1 + \cosh \theta} + \varphi^2 \frac{1 + 2 \cos \varphi}{1 + \cos \varphi} \frac{\sin \varphi}{\frac{1}{2} - \cos \varphi}}} \quad (A26)$$

Case 3. - For the plate with many lines of support running longitudinally (case 3), the stability will not be influenced by the side-edge conditions. Correspondingly, the following function is used to describe the deflection surface

$$w = \sin \frac{\pi x}{\lambda} \sum_{n=0,2,4}^{\infty} a_n \cos \frac{n\pi y}{b} \quad (A27)$$

where the origin of coordinates is taken midway between any two lines of support. Physically the problem thus considered is the buckling of an infinitely wide plate column of length λ restrained against deflection along continuous longitudinal lines which are equally spaced across the width of the plate. The stability criterion for this case is

$$\frac{\frac{4\sqrt{k}}{\pi^2 D}}{\frac{\psi b^3}{\pi^4 D} - \frac{\frac{\sin \varphi}{\varphi} - \frac{\sinh \theta}{\theta}}{1 - \cos \varphi - 1 - \cosh \theta}} \quad (A28)$$

which is the same as equation (A21) for $q = 1$, $p = \infty$.

APPENDIX B

DERIVATION OF STABILITY CRITERIA FOR CASES 4, 5, AND 6

A direct way of obtaining stability criteria for cases 4, 5, and 6 is by application of the principles of moment distribution to the stability of plates as described in reference 2. For a long plate supported along longitudinal lines by nondeflecting supports, the stability criterion is obtained by setting the sum of the stiffnesses of the members entering the joint at a given support equal to zero. The plate stiffnesses are denoted in reference 2 by the symbol S , with appropriate superscripts, and the carry over factors are given by the symbol C , with appropriate superscripts. These symbols and their superscripts will be used as defined in reference 2. The support torsional stiffnesses α and γ as defined in this paper have an absolute value four times as large as S .

Case 4. - For neutral stability, the sum of the plate stiffnesses and the support stiffness at the joint along the plate center line must equal zero. The sum of these stiffnesses is

$$\frac{1}{4} \alpha + 2S^I = 0 \quad (B1)$$

If equation (12) of reference 2 is used, equation (B1) may be written as

$$\frac{1}{4} \alpha + \frac{2S^{II}}{1 - C^2 \frac{\frac{1}{4} \gamma}{S^{II} + \frac{1}{4} \gamma}}$$

which can be put into the following nondimensional form:

$$\frac{\frac{ab}{\pi^2 D}}{1 - \frac{\frac{8}{\pi^2} \frac{S^{IIb}}{D}}{\frac{C^2}{1 + \frac{4}{\pi^2} \frac{\frac{D}{\gamma b}}{\frac{\pi^2 D}{S^{IIb}}}}}} \quad (B2)$$

Solutions to equation (B2) may be readily obtained by using the tabulated values of S^{IIb}/D and C given in reference 5.

For the particular case of simple support along the plate side edges, $\frac{\gamma_b}{\pi^2 D} = 0$, equation (B2) reduces to

$$\frac{ab}{\pi^2 D} + \frac{8}{\pi^2} \frac{S^{IIb}}{D} = 0 \quad (B3)$$

With complete fixity of the side edges, $\frac{\gamma_b}{\pi^2 D} = \infty$, equation (B2) reduces to

$$\frac{ab}{\pi^2 D} + \frac{\frac{8}{\pi^2} \frac{S^{IIb}}{D}}{1 - C^2} = 0$$

or, making use of equation (13) in reference 2 gives

$$\frac{ab}{\pi^2 D} + \frac{8}{\pi^2} \frac{Sb}{D} = 0 \quad (B4)$$

With the aid of the tabulated values of S^{IIb}/D and Sb/D given in reference 5, equations (B3) and (B4) have been plotted as curves giving the buckling-load coefficient $k = \frac{Nb^2}{\pi^2 D}$ as a function of λ/b for constant values of $ab/\pi^2 D$. These curves are presented as figures 8 and 9.

Case 5.- If the stiffnesses of the members meeting along one of the intermediate lines of support (fig. 2) is summed, the following equation for neutral stability is obtained

$$\frac{1}{4} \alpha + S^I + S^{IV} = 0 \quad (B5)$$

With S^I defined by equation (12) of reference 2, equation (B5) may be written as

$$\frac{1}{4} \alpha + \frac{S^{II}}{1 - C^2 \frac{\frac{1}{4} \gamma}{S^{II} + \frac{1}{4} \gamma}} + S^{IV} = 0$$

which can be written in the nondimensional form

$$\frac{\alpha b}{\pi^2 D} + \frac{\frac{4}{\pi^2} \frac{S^{IIb}}{D}}{1 - \frac{C^2}{\frac{S^{IIb}}{\frac{4}{\pi^2} \frac{D}{\frac{\gamma b}{\pi^2 D}}}}} + \frac{\frac{4}{\pi^2} \frac{S^{IVb}}{D}}{1 + \frac{4}{\pi^2} \frac{D}{\frac{\gamma b}{\pi^2 D}}} = 0 \quad (B6)$$

This stability criterion is readily solved by using the tabulated values of S^{IIb}/D , S^{IVb}/D , and C given in reference 5.

When $\frac{\gamma b}{\pi^2 D}$ is equal to zero, equation (B6) reduces to

$$\frac{\alpha b}{\pi^2 D} + \frac{4}{\pi^2} \left(\frac{S^{IIb}}{D} + \frac{S^{IVb}}{D} \right) = 0 \quad (B7)$$

and when $\frac{\alpha b}{\pi^2 D} = \infty$, the stability criterion is

$$\frac{\alpha b}{\pi^2 D} + \frac{4}{\pi^2} \left(\frac{S_b}{D} + \frac{S^{IVb}}{D} \right) = 0 \quad (B8)$$

Equations (B7) and (B8) have been plotted in figures 10 and 11 and are presented as curves giving the buckling-load coefficient $k = \frac{Nb^2}{\pi^2 D}$ as functions of λ/b for constant values of $ab/\pi^2 D$.

Case 6. - For a plate with many longitudinal lines of support (case 6), the condition that the stiffnesses at a joint must vanish for neutral stability is given by

$$\frac{1}{4} \alpha + 2S^{IV} = 0 \quad (B9)$$

In nondimensional form, equation (B9) may be written as

$$\frac{ab}{\pi^2 D} + \frac{8}{\pi^2} \frac{S^{IV_b}}{D} = 0 \quad (B10)$$

With the aid of the tabulated values of S^{III_b}/D given in reference 5, equation (B10) has been plotted as curves giving the buckling-load coefficient $k = \frac{Nb^2}{\pi^2 D}$ as a function of λ/b for constant values of $ab/\pi^2 D$. These curves are presented in figure 12.

REFERENCES

1. Lundquist, Eugene E., and Stowell, Elbridge Z.: Critical Compressive Stress for Flat Rectangular Plates Supported Along All Edges and Elastically Restrained Against Rotation Along the Unloaded Edges. NACA Rep. 733, 1942. (Supersedes NACA ACR, May 1941.)
2. Lundquist, Eugene E., Stowell, Elbridge Z., and Schuette, Evan H.: Principles of Moment Distribution Applied to Stability of Structures Composed of Bars or Plates. NACA Rep. 809, 1945. (Supersedes NACA WR L-326.)
3. Timoshenko, S.: Theory of Elastic Stability. McGraw-Hill Book Co., Inc., 1936, pp. 108-112.
4. Budiansky, Bernard, and Hu, Pai C.: The Lagrangian Multiplier Method of Finding Upper and Lower Limits to Critical Stresses of Clamped Plates. NACA Rep. 848, 1946. (Supersedes NACA TN 1103.)
5. Kroll, W. D.: Tables of Stiffness and Carry-Over Factor for Flat Rectangular Plates Under Compression. NACA WR L-398, 1943. (Formerly NACA ARR 3K27.)
6. Seide, Paul: The Effect of Longitudinal Stiffeners Located on One Side of a Plate on the Compressive Buckling Stress of the Plate-Stiffener Combination. NACA TN 2873, 1953.
7. Lundquist, Eugene E., and Stowell, Elbridge Z.: Restraint Provided a Flat Rectangular Plate by a Sturdy Stiffener Along an Edge of the Plate. NACA Rep. 735, 1942.
8. Schuette, Evan H., and McCulloch, James C.: Charts for the Minimum-Weight Design of Multiweb Wings in Bending. NACA TN 1323, 1947.
9. Bijlaard, P. P., and Johnston, G. S.: Compressive Buckling of Plates Due to Forced Crippling of Stiffeners. Preprint No. 408, S.M.F. Fund Paper, Inst. Aero. Sci., Jan. 1953.
10. Adams, Edwin P., and Hippisley, R. L.: Smithsonian Mathematical Formulae and Tables of Elliptic Functions. Second Reprint, Smithsonian Misc. Coll., vol. 74, no. 1, 1947.
11. Seide, Paul, and Stein, Manuel: Compressive Buckling of Simply Supported Plates With Longitudinal Stiffeners. NACA TN 1825, 1949.

TABLE I

VALUES OF DEFLECTIONAL STIFFNESS PARAMETER $\psi b^3/\pi^4 D$ FOR CASE 1

λ/b	$\psi b^3/\pi^4 D$ for $k = -$						
	0	1	2	3	4	5	6
Simply supported side edges; $\frac{\gamma b}{\pi^2 D} = 0$							
0.4	-19.89	-17.85	-15.67	-13.32	-10.71	-7.690	-3.928
.5	-10.19	-8.526	-6.680	-4.534	-1.827	2.253	12.26
.6	-5.899	-4.497	-2.861	-.7810	2.376	9.977	
.7	-3.721	-2.517	-1.050	.9544	4.558	18.79	
.8	-2.504	-1.461	-.1573	1.709	5.309	23.10	
.9	-1.773	-.8683	.2748	1.927	5.076	18.52	
1.0	-1.309	-.5230	.4676	1.877	4.411	12.58	
1.2	-.7887	-.1916	.5426	1.527	3.052	6.177	20.15
1.6	-.3826	-.0197	.3999	.9039	1.542	2.411	3.760
1.8	-.2948	-.0034	.3254	.7062	1.162	1.733	2.495
2.0	-.2384	0	.2638	.5610	.9032	1.309	1.807
2.5	-.1624	-.0081	.1571	.3353	.5293	.7427	.9803
3.0	-.1268	-.0192	.0937	.2127	.3387	.4725	.6157
4.0	-.0956	-.0349	.0275	.0917	.1580	.2263	.2970
6.0	-.0754	-.0488	-.0215	.0062	.0342	.0626	.0914
8.0	-.0688	-.0542	-.0389	-.0235	-.0080	.0076	.0233
10.0	-.0672	-.0568	-.0471	-.0373	-.0274	-.0175	-.0076
Clamped side edges; $\frac{\gamma b}{\pi^2 D} = \infty$							
0.4	-19.895	-17.85	-15.67	-13.33	-10.73	-7.766	-4.155
.5	-10.19	-8.541	-6.717	-4.626	-2.092	1.338	7.154
.6	-5.9169	-4.5417	-2.960	-1.079	1.417	5.371	14.86
.7	-3.723	-2.606	-1.266	.3898	2.658	6.424	16.11
.8	-2.565	-1.596	-.4663	.9286	2.818	5.828	12.499
.9	-1.4087	-1.041	-.0965	1.0513	2.555	4.777	8.863
1.0	-.7233	.0654	1.004	2.186	3.810	6.376	
1.2	-.4208	.1383	.7765	1.529	2.455	3.667	
1.4	-.3039	.1060	.5594	1.070	1.659	2.358	
1.6	-.2555	.0559	.3924	.7602	1.168	1.626	
2.0	-.4133	-.2262	-.0304	.1754	.3928	.6234	.8696
2.5	-.2231	-.0997	.0276	.1593	.2957	.4374	
3.0	-.2263	-.1416	-.0549	.0338	.1246	.2177	
4.0	-.2796	-.2330	-.1859	-.1381	-.0897	-.0408	.0088
6.0	-.2604	-.2398	-.2190	-.1982	-.1771	-.1560	-.1347
8.0	-.2542	-.2426	-.2308	-.2186	-.2074	-.1958	-.1839
10.0	-.2506	-.2438	-.2365	-.2289	-.2215	-.2159	-.2065



TABLE II

VALUES OF DEFLECTIONAL STIFFNESS PARAMETER $\psi b^3/\pi^4 D$ FOR CASE 2

λ/b	$\psi b^3/\pi^4 D$ for $k = -$						
	0	1	2	3	4	5	6
Simply supported side edges; $\frac{\gamma b}{\pi^2 D} = 0$							
0.4	-19.826	-17.744	-15.491	-13.029	-10.234	-6.927	-2.654
.5	-10.050						
.6	-5.707	-4.1853	-2.368	-.0123	3.511	10.600	
.8	-2.275	-1.1166	.3343	2.345	5.626		
1.0	-1.094	-.2287	.8404	2.263	4.4295		
1.2		.04579	.8196	1.790	3.094	19.46	
1.4		.1263	.6970	1.377	2.223	4.82	
1.6		.1417	.5747	1.0716	1.656		
2.0	-.1279	.1218	.3924	.6882	1.015	1.381	1.796
2.5		.0877	.2567	.4356	.6261	.8297	1.048
3.0	-.04899	.0624	.1780	.2982	.4236	.5545	.6915
4.0		.0325	.0964	.1597	.2284	.2968	.3667
6.0		.0085	.0365	.0648	.0933	.1221	.1513
8.0		-.000436	.0152	.0310	.0468	.0628	.0780
10.0	-.01463	-.00466	.00534	.0154	.0254	.0356	.0457
Clamped side edges; $\frac{\gamma b}{\pi^2 D} = \infty$							
0.4	-19.623	-17.745	-15.493	-13.035	-10.248	-6.963	-2.758
.5		-8.348	-6.327	-3.980	-.9679	3.466	
.6	-5.5807	-4.206	-2.418	-.1383	3.178	10.118	
.8	-2.1971	-1.173	.2171	2.107	5.371		
1.0	-1.0593	-.3041	.7094	2.0576			
1.2	-.5948	-.0334	.70025	1.630	3.031		
1.4	-.3772	.0494	.5919	1.247	2.122		
1.6	-.2637	.0686	.4813	.9603	1.550		
2.0	-.1602	.0554	.3143	.5995	.9209	1.296	1.767
2.5		.0268	.1890	.3614	.5464	.7475	.9689
3.0		.00478	.1159	.2317	.3530	.4807	.6158
4.0	-.07566	-.0215	.0399	.1030	.1673	.2334	.3013
6.0	-.06696	-.0430	-.0160	.0113	.0388	.0666	.0947
8.0		-.0513	-.0358	-.0207	-.00540	.00996	.0243
10.0	-.06336	-.0544	-.0451	-.0353	-.0257	-.0159	-.00619



TABLE III
VALUES OF DEFLECTIONAL STIFFNESS PARAMETER $\psi b^3/\pi^4 D$ FOR CASE 3

λ/b	$\psi b^3/\pi^4 D$ for $k = -$					
	0	1	2	3	4	5
0.4	-19.758	-17.622	-15.304	-12.730	-9.775	-6.197
.5	-9.915	-8.076	-5.955	-3.381	0	5.072
.6	-5.524	-3.895	-1.922	.6415	4.366	10.935
.7	-3.297	-1.861	-.0828	2.291	5.851	
.8	-2.064	-.8232	.7235	2.720	5.915	
1.0	-.9180	0	1.1066	2.502		
1.2	-.4600	.2169	1.004	1.957	3.104	
1.4		.2570	.8317	1.490	2.260	
1.6		.1919	.4626	.7525	1.065	1.402
2.0	-.06203	.1367	.3059	.4827	.6678	.8621
2.5		.1000	.2158	.3351	.4582	.5854
3.0	-.01234	.05905	.1231	.1882	.2544	.3219
4.0	-.003909	.03860	.07923	.1203	.1618	.2038
5.0		.02710	.05519	.08349	.1120	.1407
6.0	-.000769	.01541	.03114	.04693	.06278	.07871
8.0	-.000243	.009913	.01995	.03002	.04012	.05024
10.0	-.00010					.06039

TABLE IV
VALUES OF FUNCTIONS APPEARING IN THE STABILITY CRITERIA

λ/b	φ	$\sin \varphi$	$\cos \varphi$	θ	$\sinh \theta$	$\cosh \theta$
$k = 1$						
0.4	6.08371	219.331	219.33	9.2929	5430.37	5430.37
.5	4.44291	42.5051	42.517	7.6953	1099.01	1099.01
.6	3.31151	13.6951	13.731	6.6231	376.14	376.14
.7	2.45821	5.79911	5.8846	5.8516	173.89	173.90
.8	1.75621	2.80881	2.9815	6.2686	97.070	97.075
.9	1.10381	1.34201	1.6736	4.8115	61.454	61.462
1.0	0	0	1.0	4.4429	42.505	42.517
1.2	1.1708	.92106	.38941	3.8831	24.277	24.298
1.4	1.4192	.98853	.15102	3.4764	16.156	16.187
1.6	1.5209	.99875	.04987	3.1660	11.835	11.877
2.0	1.5708	1.0	0	2.7207	7.5626	7.6277
2.5	1.5391	.99950	.03169	2.3510	5.2004	5.2957
3.0	1.4810	.99597	.08967	2.0944	3.9987	4.1218
4.0	1.3604	.97795	.20885	1.7562	2.8089	2.9815
6.0	1.1708	.92106	.38941	1.3853	1.8729	2.1231
8.0	1.0390	.86190	.50708	1.1781	1.4702	1.7780
10.0	.9425	.80903	.58777	1.0419	1.2409	1.5937
$k = 2$						
0.4	5.17601	88.4851	88.491	9.8275	9268.36	9268.36
.5	3.40041	14.9711	15.007	8.2094	1837.67	1837.67
.6	2.03781	3.77171	3.9020	7.1189	617.54	617.54
.7	.449921	.465251	1.1029	6.3310	280.86	280.86
.8	1.4233	.98914	.14696	5.7331	154.46	154.46
.9	1.8232	.96831	-.24973	5.2619	96.422	96.427
1.0	2.0219	.89996	-.43595	4.8813	65.897	65.905
1.2	2.1858	.81677	-.57696	4.2995	36.825	36.838
1.4	2.2213	.79577	-.60558	3.8737	24.050	24.071
1.6	2.2064	.80471	-.59366	3.5467	17.335	17.364
2.0	2.1240	.85084	-.52541	3.0735	10.786	10.832
2.5	2.0010	.90888	-.41705	2.6762	7.2305	7.2993
3.0	1.8857	.95082	-.30972	2.3977	5.4534	5.5444
4.0	1.6949	.99231	-.12379	2.0264	3.7275	3.8593
6.0	1.4325	.99045	.13786	1.6126	2.4082	2.6076
8.0	1.2612	.95246	.30467	1.3780	1.8574	2.1095
10.0	1.1389	.90817	.41859	1.2225	1.5506	1.8451



TABLE IV

VALUES OF FUNCTIONS APPEARING IN THE STABILITY CRITERIA - Continued

λ/b	φ	$\sin \varphi$	$\cos \varphi$	θ	$\sinh \theta$	$\cosh \theta$
$k = 3$						
0.4	4.35301	38.8501	38.862	10.219	13720.4	13720.4
.5	2.29981	4.93591	5.0362	8.5831	2670.3	2670.3
.6	1.0371	.86093	.50872	7.4771	883.56	883.56
.7	2.0685	.87868	-.47741	6.6756	396.42	396.42
.8	2.4387	.64643	-.76297	6.0654	215.35	215.35
.9	2.6095	.50733	-.86174	5.5838	133.04	133.04
1.0	2.6879	.43829	-.89883	5.1927	89.975	89.981
1.2	2.7188	.41031	-.91195	4.5934	49.410	49.421
1.4	2.6786	.44663	-.89472	4.1528	31.798	31.814
1.6	2.6132	.50415	-.86362	3.8131	22.634	22.657
2.0	2.4658	.62551	-.78021	3.3188	13.796	13.832
2.5	2.2932	.75022	-.66119	2.9012	9.0705	9.1255
3.0	2.1451	.83957	-.54325	2.6067	6.7402	6.8140
4.0	1.9122	.94229	-.33481	2.2115	4.5099	4.6195
6.0	1.6047	.99943	-.03390	1.7673	2.8421	3.0129
8.0	1.4081	.98679	.16198	1.5136	2.1615	2.3816
10.0	1.2692	.95486	.29666	1.3447	1.7882	2.0488
$k = 4$						
0.4	3.51241	16.7501	16.779	10.537	18864.3	18864.3
.5	0	0	1.0	8.8858	3614.34	3614.34
.6	2.3416	.71735	-.69671	7.77662	1179.76	1179.76
.7	2.8385	.29847	-.95442	6.9528	523.04	523.04
.8	3.0418	.09963	-.99502	6.3321	281.17	281.17
.9	3.1221	.01949	-.99980	5.8410	172.06	172.06
1.0	3.1416	0	-1.0	5.4414	115.381	115.385
1.2	3.0976	.04398	-.99902	4.8273	62.433	62.441
1.4	3.0106	.13062	-.99143	4.3733	39.690	39.703
1.6	2.9123	.22729	-.97383	4.0240	27.953	27.971
2.0	2.7207	.40857	-.91272	3.5124	16.750	16.779
2.5	2.5133	.58776	-.80903	3.0781	10.836	10.882
3.0	2.3416	.71735	-.69671	2.7706	7.9528	8.0154
4.0	2.0780	.87411	-.48573	2.3562	5.2280	5.3228
6.0	1.7366	.98629	-.16505	1.8879	3.2270	3.3784
8.0	1.5209	.99876	.049876	1.6191	2.4252	2.6233
10.0	1.3694	.97979	.20004	1.4397	1.9912	2.2282

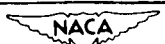


TABLE IV

VALUES OF FUNCTIONS APPEARING IN THE STABILITY CRITERIA - Concluded

λ/b	φ	$\sin \varphi$	$\cos \varphi$	θ	$\sinh \theta$	$\cosh \theta$
$k = 5$						
0.4	2.5519i	6.37681	6.4547	10.810	24768.18	24768.18
.5	2.1587	.83210	-.55462	9.1442	4680.05	4680.05
.6	3.0604	.08110	-.99670	8.0123	1508.94	1508.94
.7	3.3742	-.23051	-.97306	7.1881	661.798	661.798
.8	3.4879	-.33942	-.94062	6.5580	352.43	352.43
.9	3.5123	-.36227	-.93206	6.0585	213.87	213.87
1.0	3.4928	-.34403	-.93895	5.6514	142.34	142.35
1.2	3.3967	-.25235	-.96763	5.0244	76.037	76.044
1.4	3.2754	-.13341	-.99105	4.5606	47.815	47.826
1.6	3.1524	-.01081	-.999932	4.2010	33.369	33.384
2.0	2.9270	.21295	-.97706	3.6745	19.702	19.727
2.5	2.6923	.43433	-.90075	3.2260	12.570	12.609
3.0	2.5019	.59695	-.80228	2.9074	9.1272	9.1819
4.0	2.2137	.80036	-.59952	2.4767	5.9090	5.9930
6.0	1.8450	.96264	-.27078	1.9881	3.5823	3.7193
8.0	1.6138	.99908	-.042990	1.7067	2.6646	2.8461
10.0	1.4520	.99259	.11852	1.5184	2.1729	2.3920
$k = 6$						
0.4	1.1164i	1.36321	1.6906	11.051	31542.81	31542.81
.5	2.9787	.16217	-.98676	9.3718	5872.07	5872.07
.6	3.5885	-.43217	-.90178	8.2285	1873.12	1873.12
.7	3.7940	-.60709	-.79461	7.3945	813.515	813.515
.8	3.8468	-.64818	-.76147	6.7558	429.518	429.518
.9	3.8311	-.63615	-.77155	6.2487	258.67	258.67
1.0	3.7823	-.59776	-.80167	5.8348	171.00	171.00
1.2	3.6459	-.48319	-.87550	5.1962	90.291	90.296
1.4	3.4975	-.34844	-.93732	4.7227	56.232	56.241
1.6	3.3548	-.21159	-.97734	4.3549	38.923	38.936
2.0	3.1017	.039882	-.99920	3.8151	22.680	22.702
2.5	2.8445	.29274	-.95619	3.3540	14.291	14.326
3.0	2.6385	.48214	-.87609	3.0257	10.280	10.329
4.0	2.3296	.72566	-.68805	2.5808	6.5660	6.6417
6.0	1.9378	.93341	-.35882	2.0745	3.9175	4.0431
8.0	1.6934	.99249	-.12230	1.7822	2.8873	3.0556
10.0	1.5228	.99885	.047978	1.5863	2.3405	2.5452



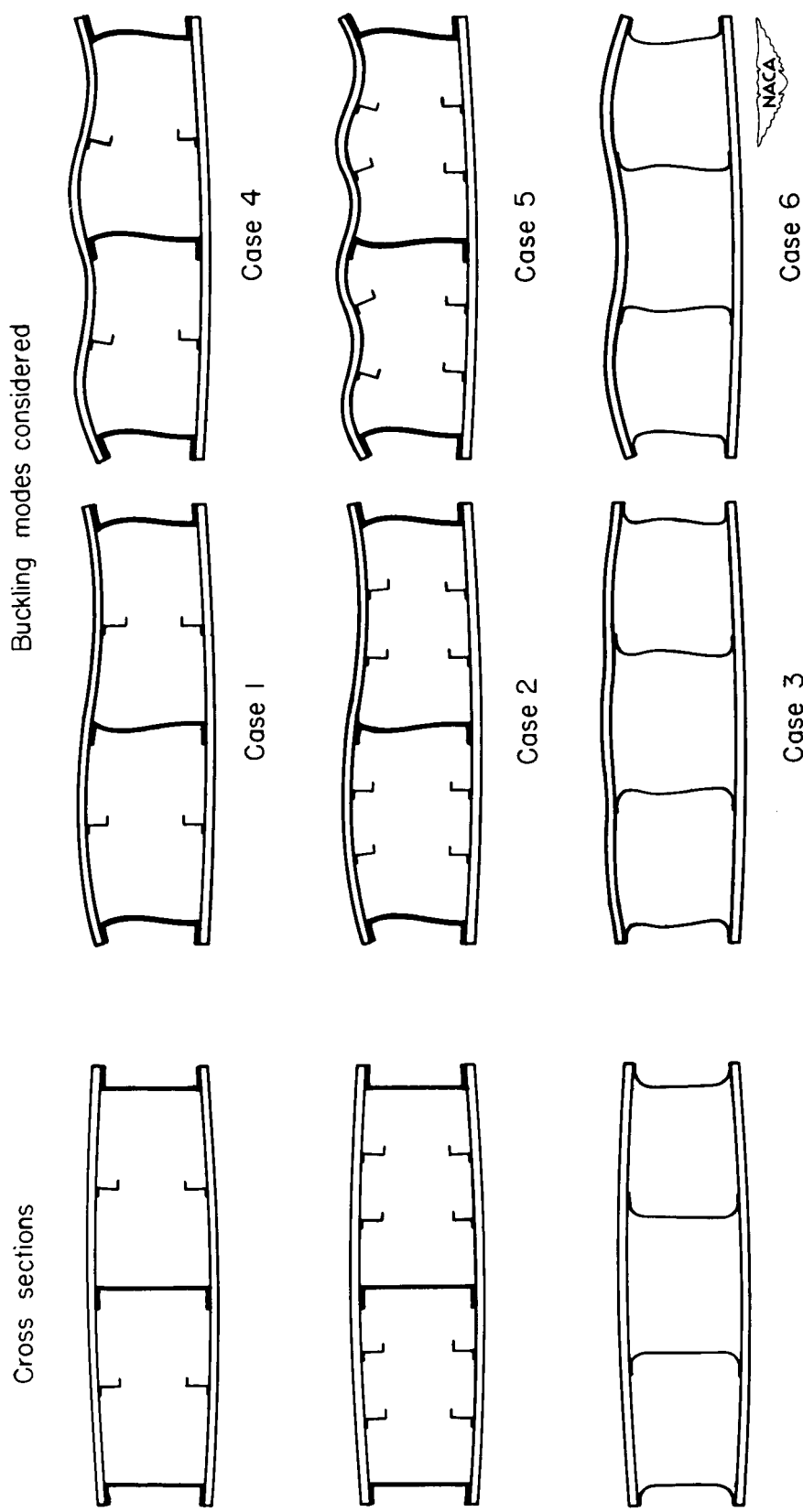
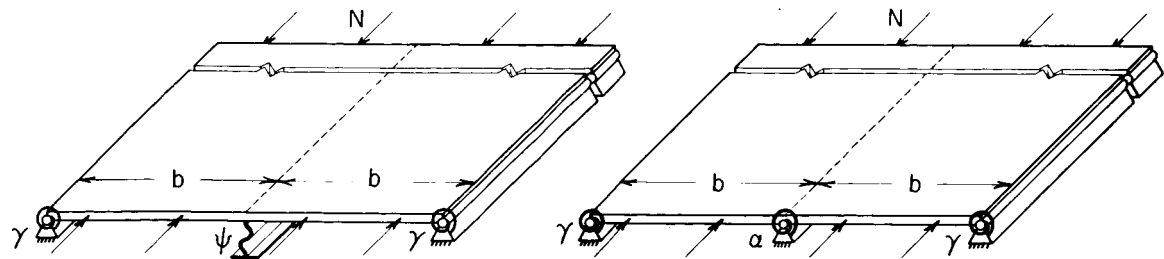
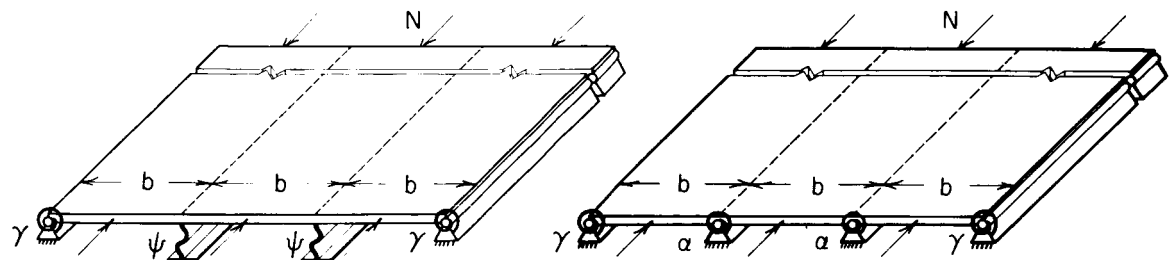


Figure 1.- Thick-skin box-beam cross sections and the buckling modes considered for each.



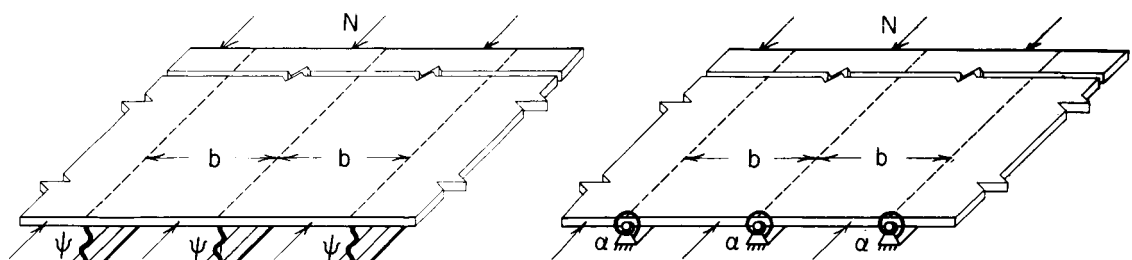
Case 1

Case 4



Case 2

Case 5



Case 3

Case 6



Figure 2.- Six cases for which stability criteria are presented.

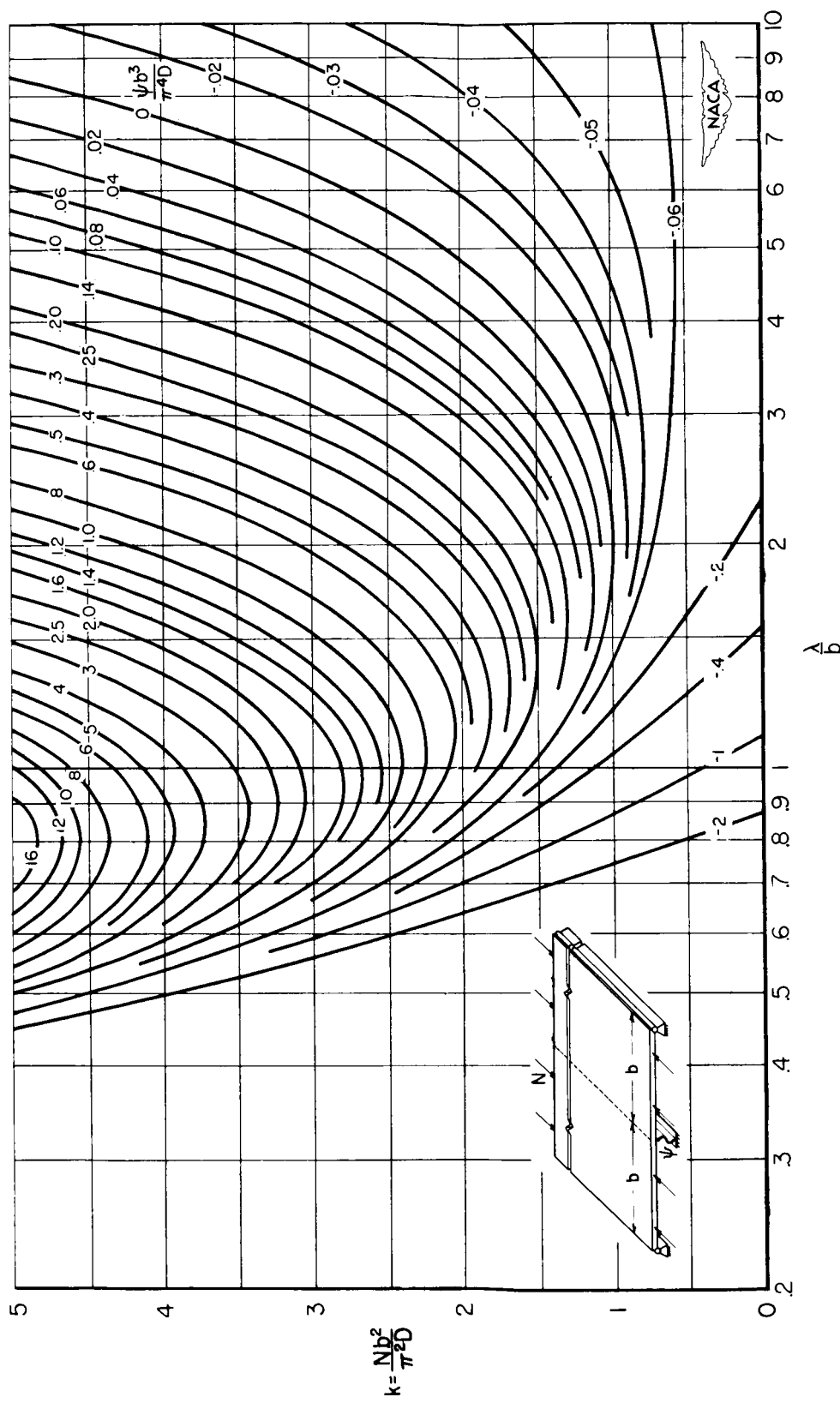


Figure 3.- Stability curves for case 1 with simply supported side edges.

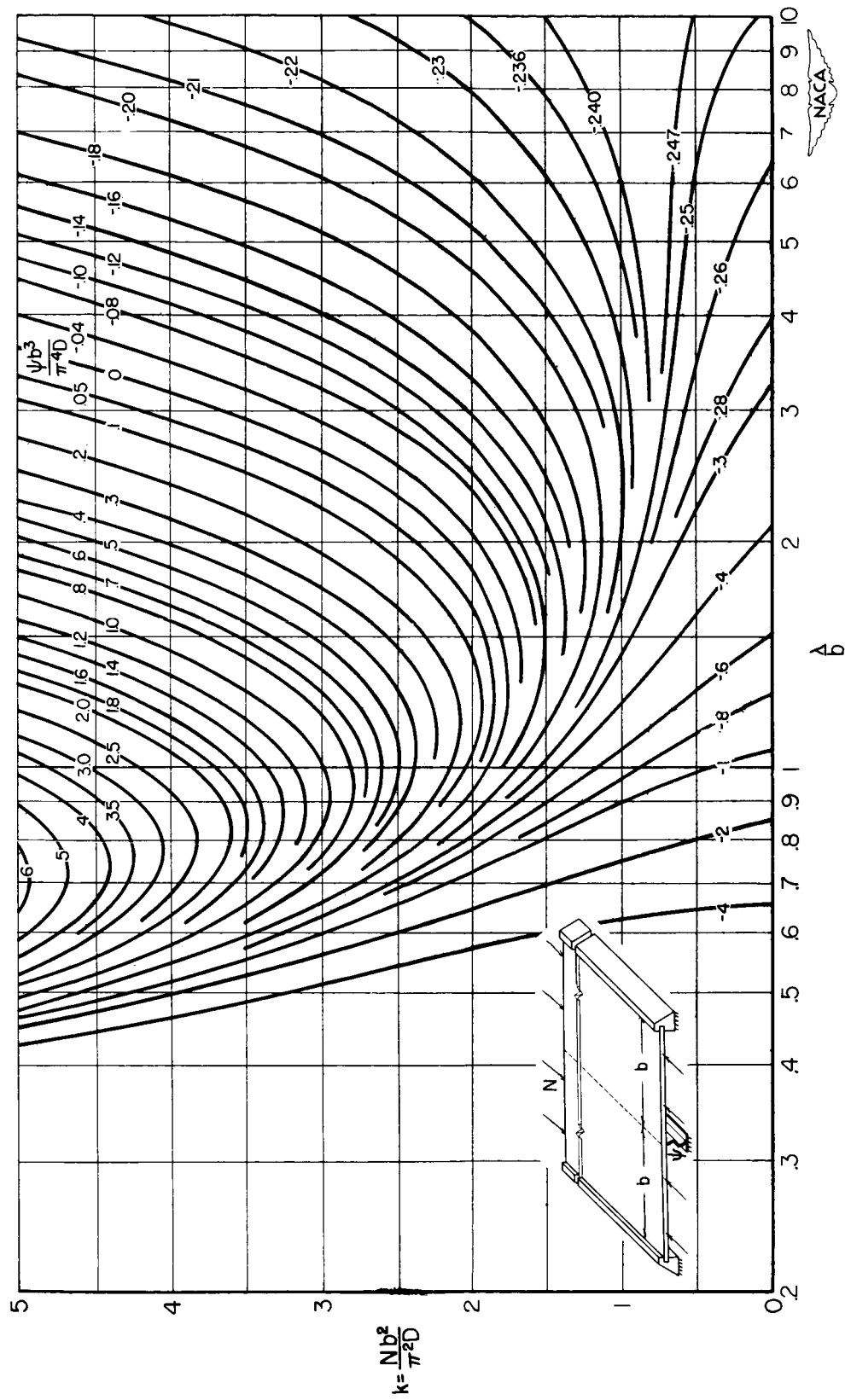


Figure 4.- Stability curves for case 1 with clamped side edges.

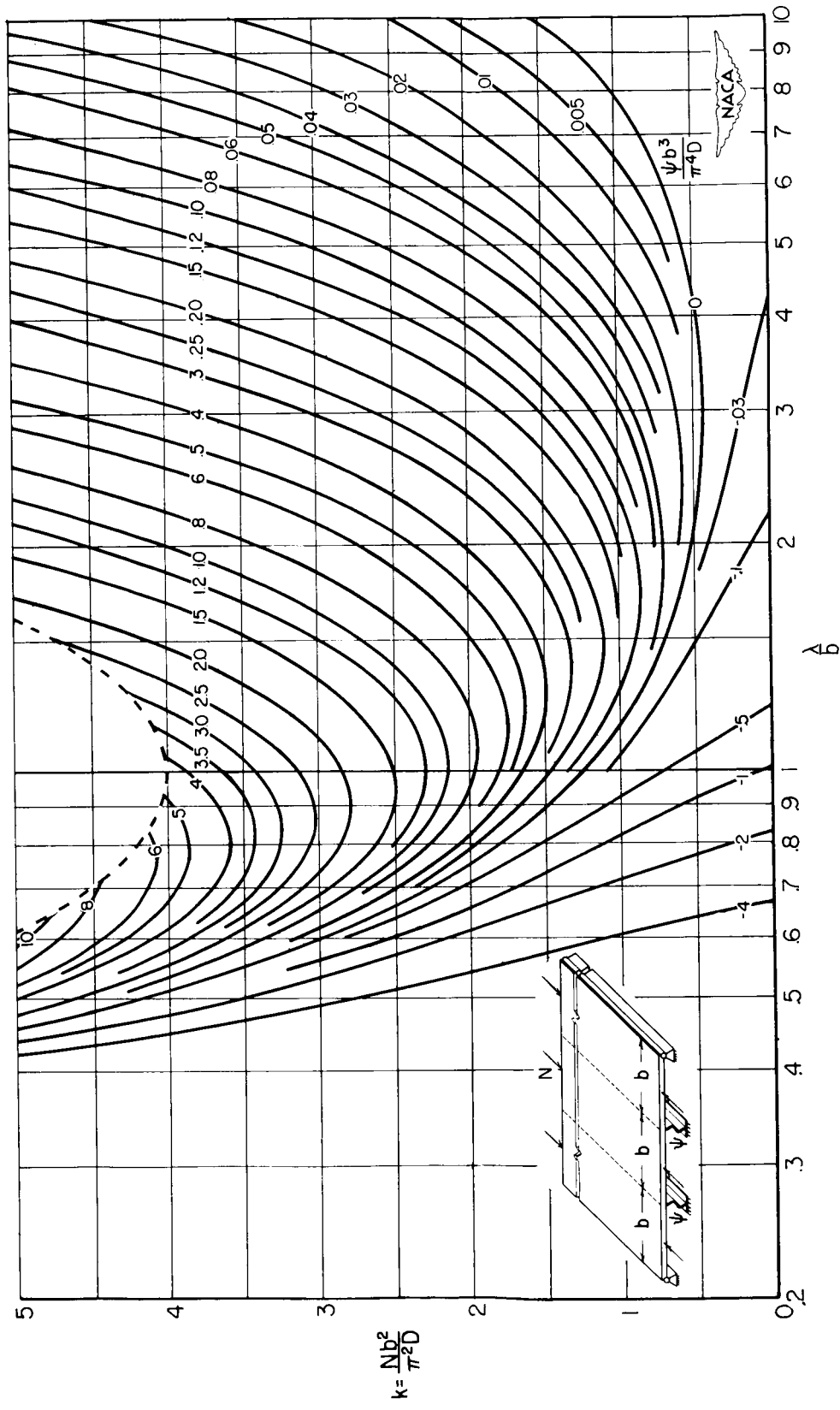


Figure 5.- Stability curves for case 2 with simply supported side edges.

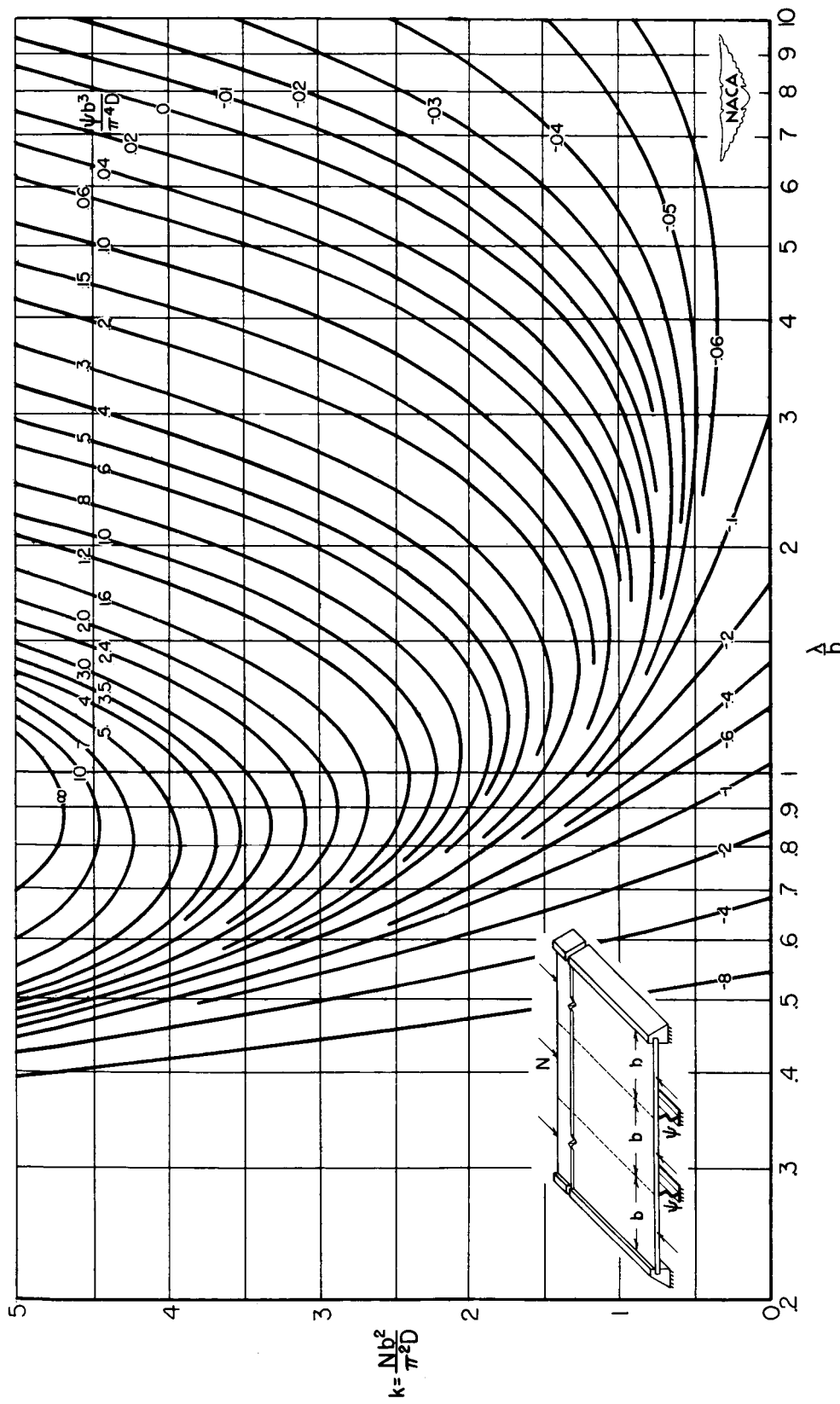


Figure 6.- Stability curves for case 2 with clamped side edges.

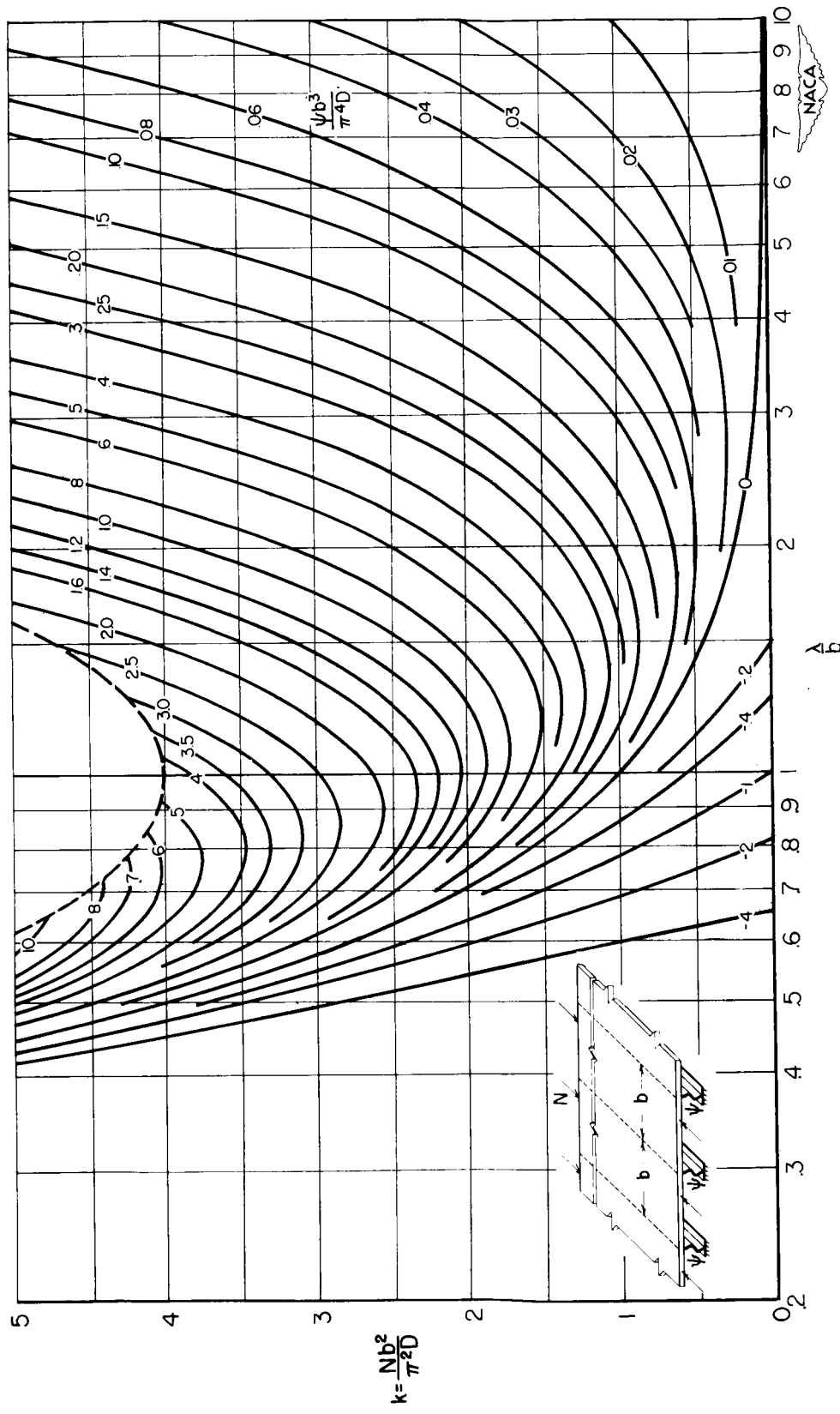


Figure 7.- Stability curves for case 3.

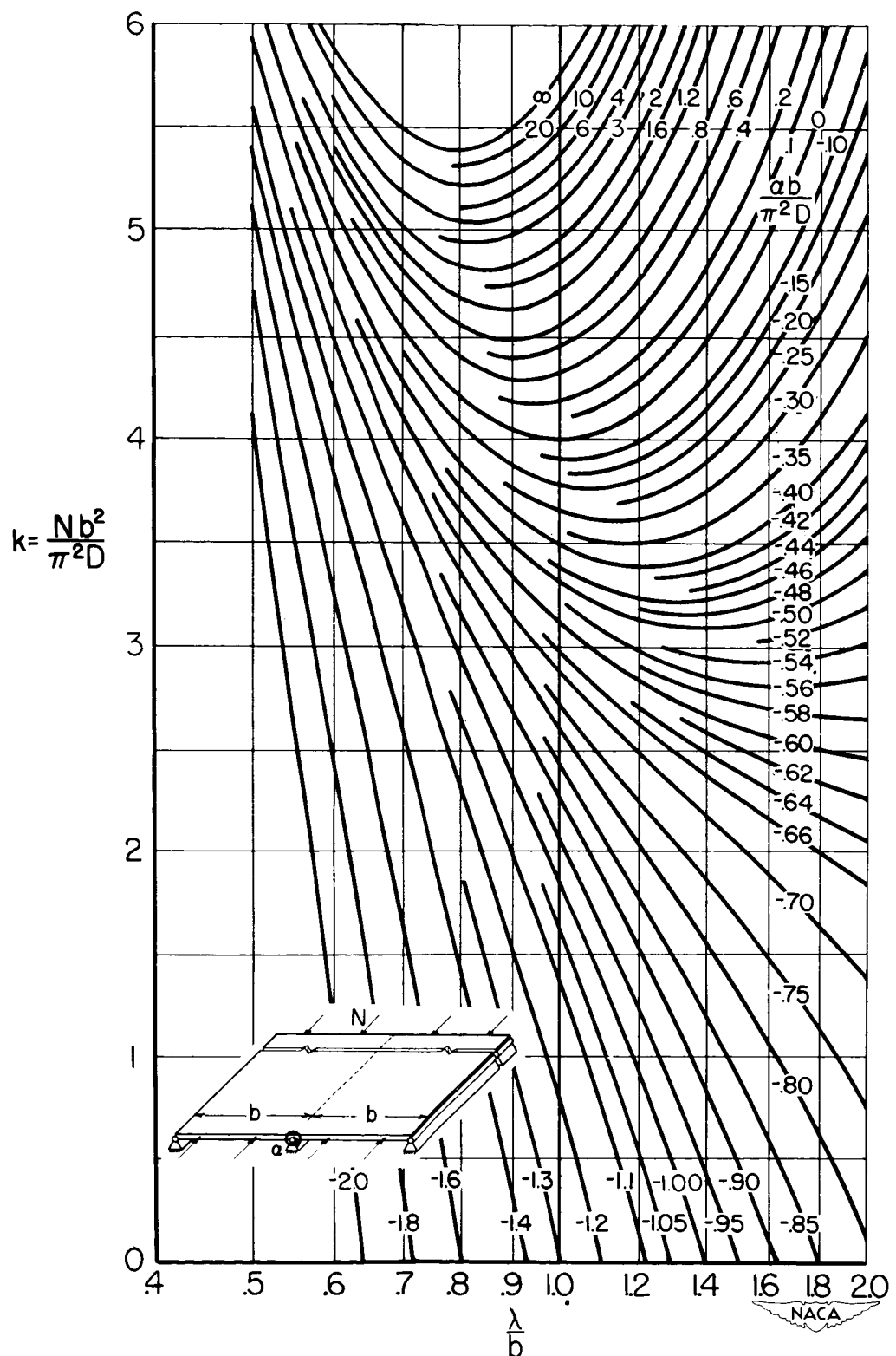


Figure 8.- Stability curves for case 4 with simply supported side edges.

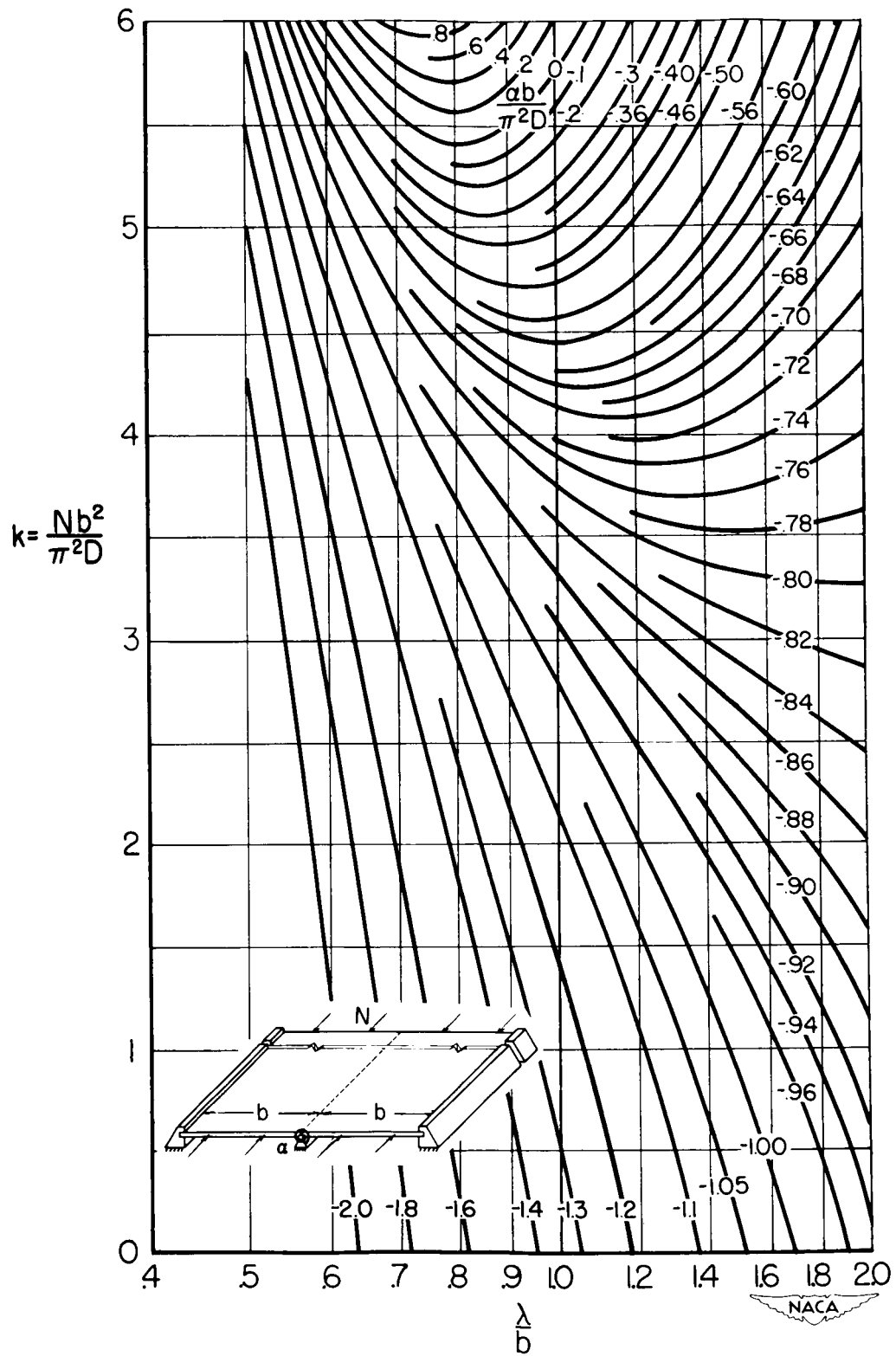


Figure 9.- Stability curves for case 4 with clamped side edges.

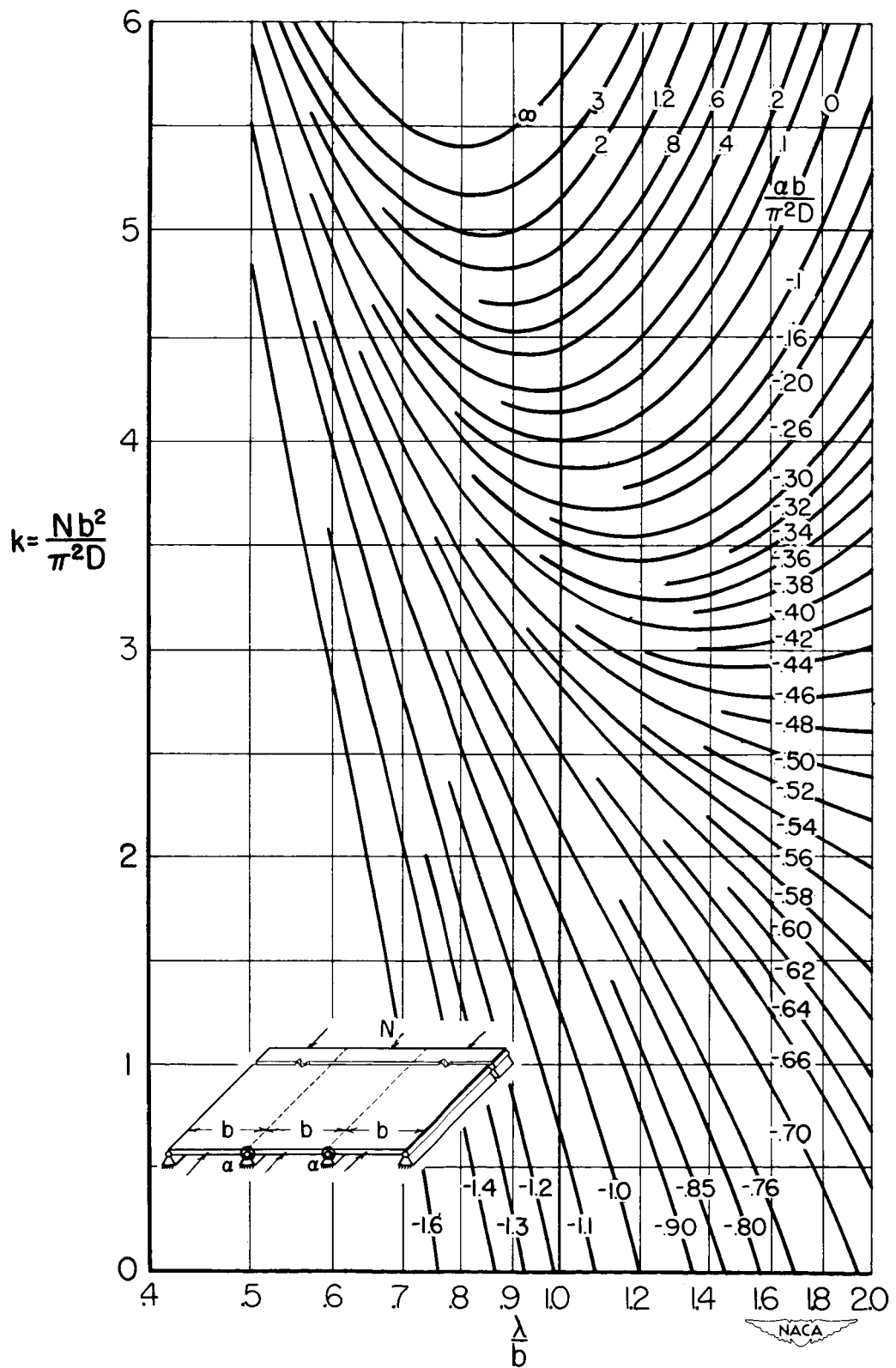


Figure 10.- Stability curves for case 5 with simply supported side edges.

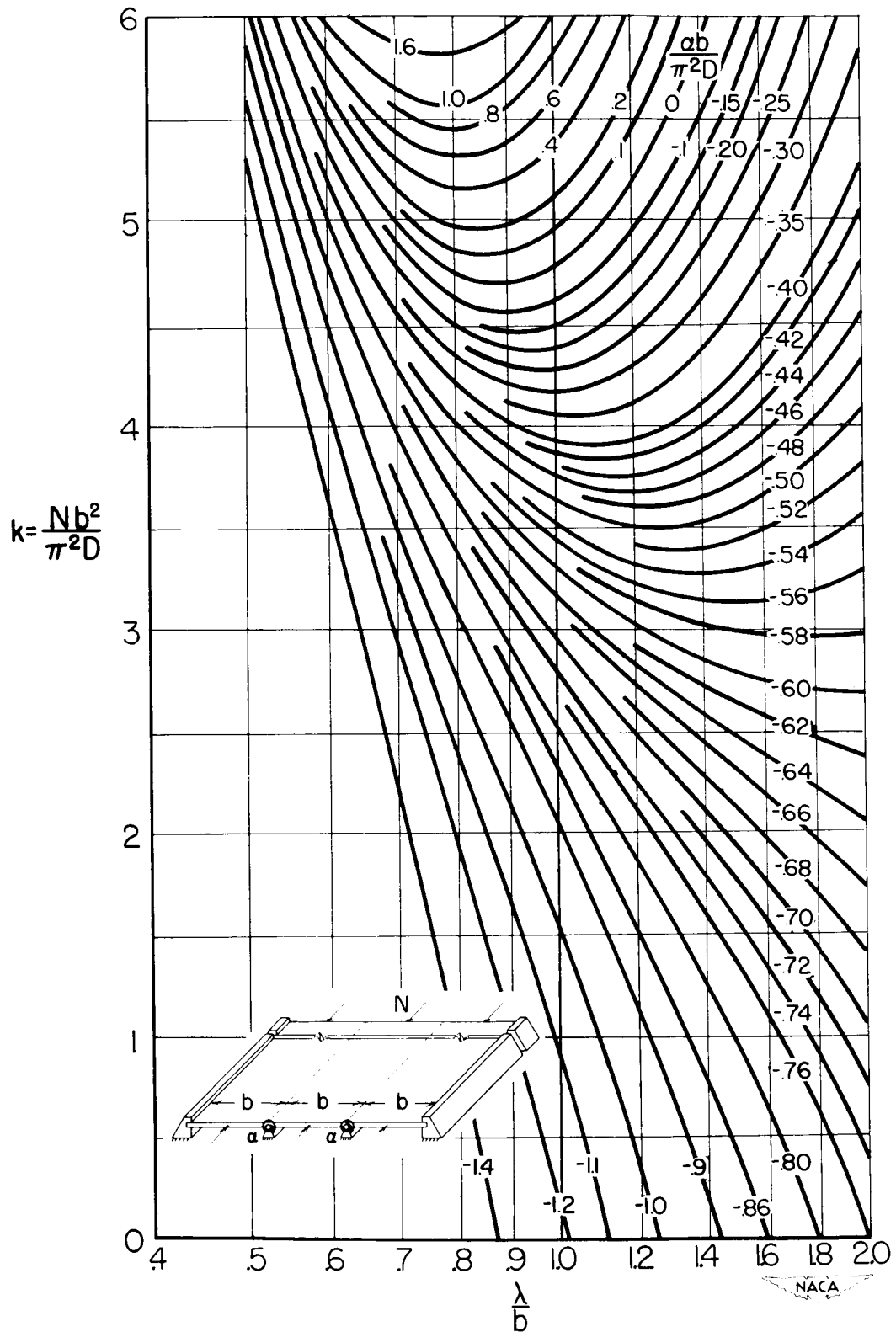


Figure 11.- Stability curves for case 5 with clamped side edges.

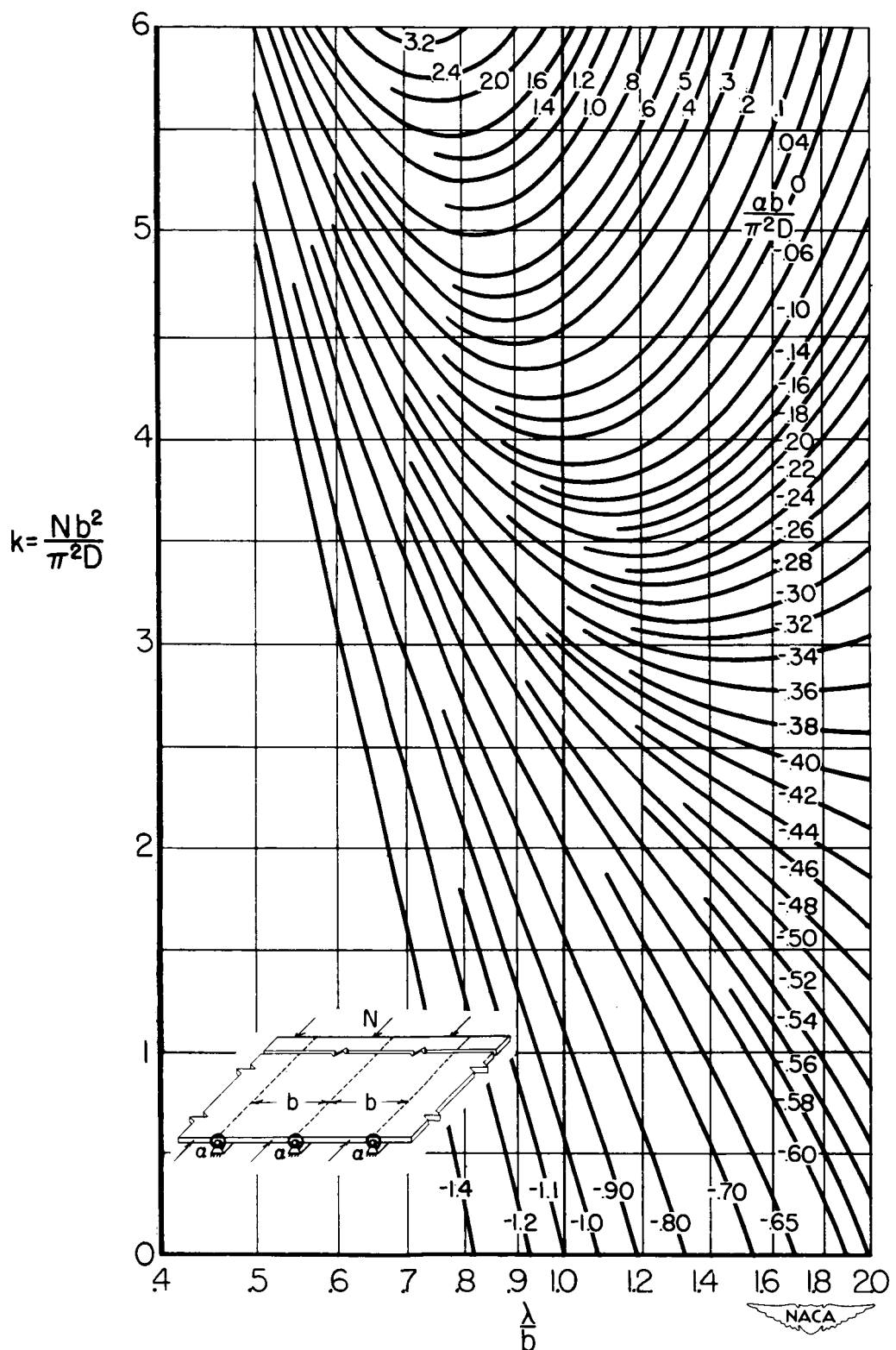


Figure 12.- Stability curves for case 6.

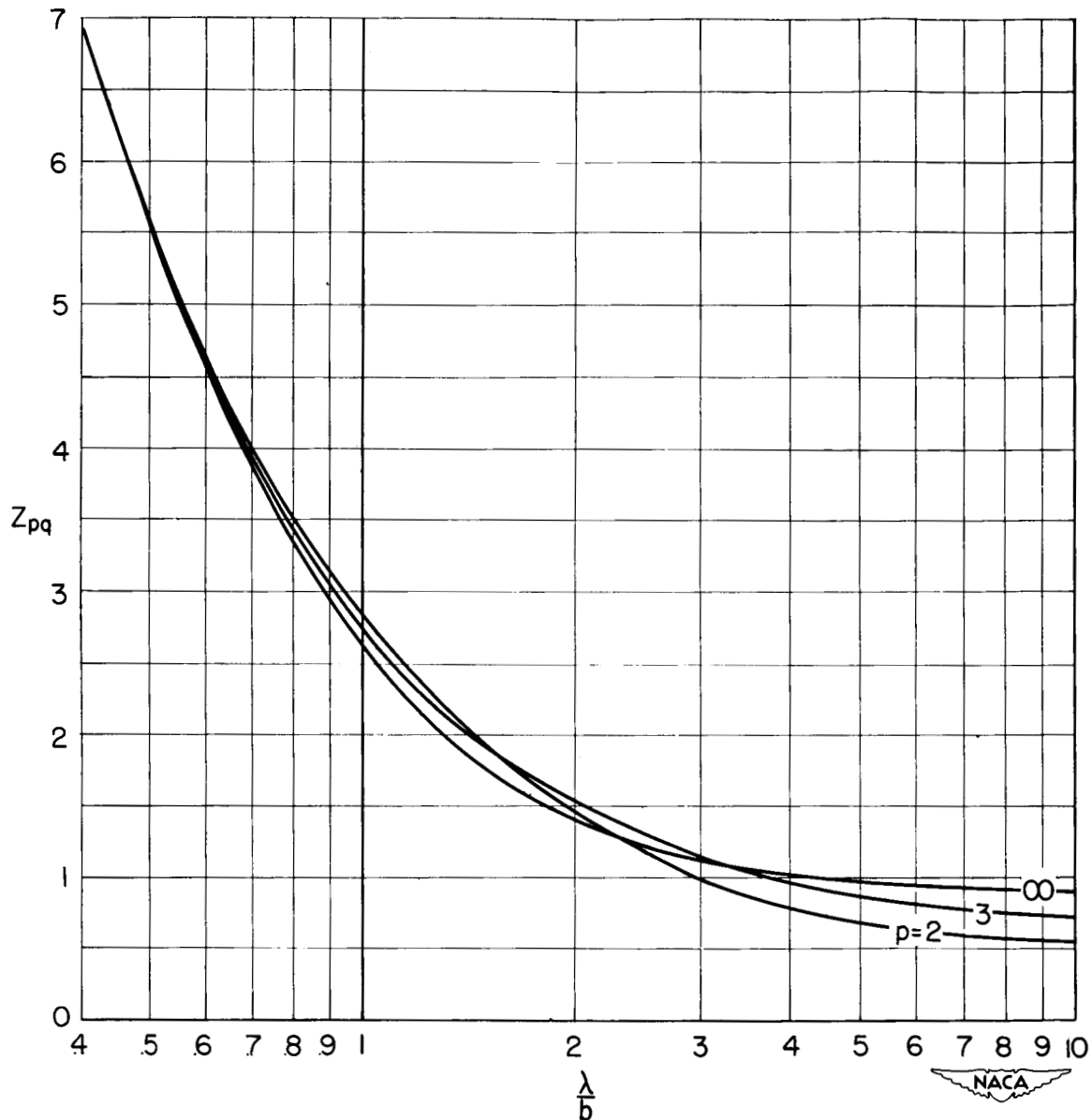
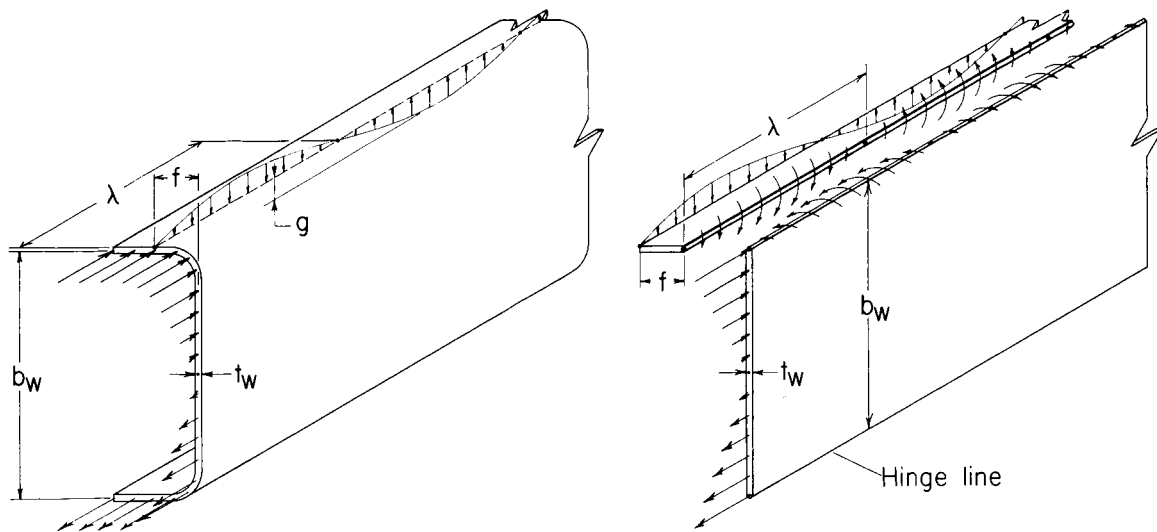
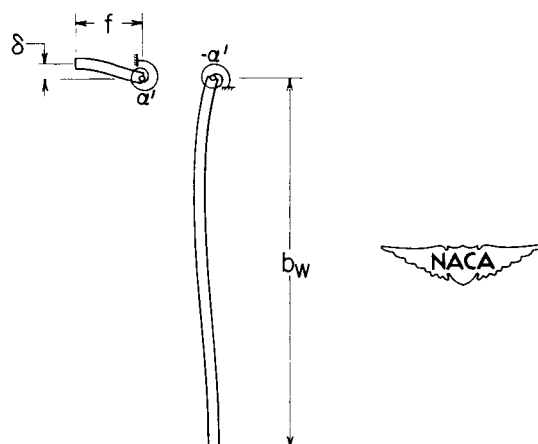


Figure 13.- Functions appearing in expression for effective flexural stiffness of stiffeners attached to one side of plate (from ref. 6).



(a) Loads on web.

(b) Idealization of web.



(c) Deformed shape of idealized web.

Figure 14.- Loads and deformations used in calculating the effective stiffness of channel-type full-depth webs.